

# Thermal one point functions, large $d$ and interior geometry of black holes

Justin R. David and Srijan Kumar

*Centre for High Energy Physics, Indian Institute of Science,  
C.V. Raman Avenue, Bangalore 560012, India*

*E-mail:* [justin@iisc.ac.in](mailto:justin@iisc.ac.in), [srijankumar@iisc.ac.in](mailto:srijankumar@iisc.ac.in)

**ABSTRACT:** We study thermal one point functions of massive scalars in  $AdS_{d+1}$  black holes. These are induced by coupling the scalar to either the Weyl tensor squared or the Gauss-Bonnet term. Grinberg and Maldacena argued that the one point functions sourced by the Weyl tensor exponentiate in the limit of large scalar masses and they contain information of the black hole geometry behind the horizon. We observe that the one point functions behave identically in this limit for either of the couplings mentioned earlier. We show that in an appropriate large  $d$  limit, the one point function for the charged black hole in  $AdS_{d+1}$  can be obtained exactly. These black holes in general contain an inner horizon. We show that the one point function exponentiates and contains the information of both the proper time between the outer horizon to the inner horizon as well as the proper length from the inner horizon to the singularity. We also show that Gauss-Bonnet coupling induced one point functions in  $AdS_{d+1}$  black holes with hyperbolic horizons behave as anticipated by Grinberg-Maldacena. Finally, we study the one point functions in the background of rotating BTZ black holes induced by the cubic coupling of scalars.

**KEYWORDS:** AdS-CFT Correspondence, Black Holes, Thermal Field Theory

**ARXIV EPRINT:** [2212.07758](https://arxiv.org/abs/2212.07758)

---

**Contents**

<b>1</b>	<b>Introduction</b>	<b>1</b>
<b>2</b>	<b>Gauss-Bonnet induced thermal one point function</b>	<b>3</b>
<b>3</b>	<b>The charged planar black hole at large <math>d</math></b>	<b>8</b>
<b>4</b>	<b>Hyperbolic black holes</b>	<b>14</b>
<b>5</b>	<b>BTZ black holes with angular momentum</b>	<b>18</b>
5.1	Thermal one point function from gravity	20
5.2	One point function $\langle O^2 \rangle$ from CFT	27
<b>6</b>	<b>Conclusions</b>	<b>30</b>
<b>A</b>	<b>Details for the Green's function</b>	<b>30</b>
<b>B</b>	<b>The charged planar black hole solution at large <math>d</math></b>	<b>32</b>
<b>C</b>	<b>Large <math>d</math> with Weyl tensor squared coupling</b>	<b>33</b>

---

**1 Introduction**

The physics of the horizon of black holes and the geometry behind the horizon have continued to be problems of interest in quantum gravity. The AdS/CFT correspondence [1] in principle gives us a handle to study the geometry behind the horizon using boundary correlators of the CFT at finite temperature. Studies in this direction were initiated some time ago by approximating 2-point functions of massive scalars in terms of space like geodesics in the large mass limit [2]. Recently Grinberg and Maldacena [3] have argued in general that even one point functions of massive scalars in  $AdS_{d+1}$  black hole geometries contain some information of the geometry behind the horizon. This has been investigated further in [4–7].

One point functions in holographic backgrounds have been studied earlier to establish sum-rules and high frequency behaviour of transport coefficients [8–10]. Using an example studied by [10], Grinberg and Maldacena observe the thermal one point function in the planar  $AdS_{d+1}$  Schwarzschild black hole evaluated for scalars dual to operators of low dimensions can be analytically continued to large operator dimensions. When this is done, the thermal one point function exponentiates and one can read out the proper time to singularity from the event horizon. The one point function is sourced by the coupling of the scalar to the Weyl tensor squared term. Using the intuition from this exactly solvable

example, [3] developed a saddle point approximation for large masses. The saddle involved geodesics at complex radial positions and arguments justifying the location of the saddle and the contour involved in the WKB approximation. One of the interesting claims of their saddle point analysis is that for the  $AdS_5$  charged black hole which has an inner horizon, the one point function exponentiates to the form

$$\langle \mathcal{O} \rangle \sim \exp(-m(\ell_{\text{hor}} + \ell_{\text{sing}} - i\tau_{\text{in}})) . \tag{1.1}$$

Here  $\tau_{\text{in}}$  is the proper time for a particle to reach the inner horizon from the outer horizon,  $\ell_{\text{hor}}$  is the regularized proper length from the boundary to the outer horizon and  $\ell_{\text{sing}}$  is the proper length from the inner horizon to the singularity. The lengths are shown on the Penrose diagram of the charged black hole in figure 2. In this analysis, the massive scalar field is taken to be a probe and its back reaction is neglected. One of the aims of this paper is to provide a solvable example similar to the  $AdS_{d+1}$  Schwarzschild black hole to show indeed that the expectation value of the thermal one point functions in the charged black hole indeed exponentiates as in (1.1).

In this paper we study one point functions of massive scalars sourced by the Gauss-Bonnet curvature as well as the Weyl tensor squared. For the solvable case of planar Schwarzschild black hole we see that the result for the thermal one point function sourced by the Gauss-Bonnet curvature is identical to that of the Weyl tensor squared term. We then present examples in which the one point function of massive scalars can be exactly obtained for small conformal dimensions just as the example seen first in [10] for the  $AdS_{d+1}$  Schwarzschild black hole. The first example is the planar charged black hole in  $AdS_{d+1}$  in a suitable large  $d$  limit. Large  $d$  limit has been studied earlier by several groups, see [11] for a recent review. The large  $d$  limit used in this paper also involves a simultaneous limit on the charge of the black hole, which is distinct from that discussed in [11].<sup>1</sup> We see that the one point function can be obtained exactly and it exponentiates for large scalar masses just as expected by arguments in [3]. We show that the one can read out all the 3 lengths in (1.1) from the one point function. We also observe that this result is independent of whether the one point function is sourced by Gauss-Bonnet curvature or the Weyl tensor squared.

The second example we study are the black holes with hyperbolic horizons in  $AdS_{d+1}$ . Here we show that the Gauss-Bonnet curvature sources one point function which again behave as anticipated by [3]. We can read out the  $\tau_s$ , the proper time from the horizon to the singularity from the one point function. The dependence of  $\tau_s$  on the AdS radius is different from Schwarzschild black holes with planar horizons. Therefore this example serves another check of the general arguments of [3].

Finally we study the one point functions in the background of the rotating BTZ black hole. By conformal invariance, thermal one point functions of primaries vanish in  $2d$  CFT's on a line. However if the spatial directions are periodic, they acquire non-trivial expectation values. Holographically these one point functions are sourced due to cubic couplings of the

---

<sup>1</sup>See the recent work of [12] for another instance in which holographic observables are exactly solvable in a large  $d$  limit.

massive scalar with other scalars in the theory [13]. The auxiliary scalar sources the scalar of interest due to the non-trivial windings around the circular horizon of the BTZ. These one point functions were explored for the non-rotating BTZ in [3]. As expected, they decay exponentially as  $\exp(-\frac{2\pi L}{\beta})$ , where  $L$  is size of the spatial identifications. However, from the coefficient of this leading term, we can extract the proper time to singularity. We generalize this computation to the rotating BTZ and obtain the exact one point function sourced due to the cubic coupling of scalars. We then take a limit which retains the information of the inner horizon, it is possible to interpret the coefficient of  $\exp(-\frac{2\pi L}{\beta})$  geometrically. From this coefficient, we see that we can read out both  $\tau_s$  and  $\ell_{\text{hor}}$ , but there is no dependence on  $\ell_{\text{sing}}$ . We verify that this behaviour is also exhibited by the expectation value of composite operators  $\langle \mathcal{O}^2 \rangle$  of large integer scaling dimensions in finite temperature 2d CFT. The WKB type arguments used in [3] assumed radial symmetry. It will be interesting to generalize those arguments to the case of rotating black holes in higher dimensions and as well try to obtain the thermal one point functions exactly to see if they behave as in (1.1).

The organization of the paper is as follows. In section 2, we evaluate the one point function of massive scalars in the planar Schwarzschild black hole in  $AdS_{d+1}$  sourced by the Gauss-Bonnet coupling, we observe that the result for the one point function is identical to that of the Weyl-tensor squared coupling. In section 3, we repeat the analysis for charged planar black holes in  $AdS_{d+1}$  in a suitable large  $d$  limit. Section 4 contains the evaluation of the one point function in hyperbolic black holes. In section 5 we study the thermal one point function sourced by cubic coupling of scalars in the rotating BTZ black hole. Section 6 has our conclusions. Appendix A has details regarding the evaluation of the Greens functions needed to evaluate the thermal one point function. Appendix B discusses the details of the planar charged black hole in  $AdS_{d+1}$  in the large  $d$  limit developed in the paper. Appendix C shows that the result for the one point function sourced by the Weyl tensor squared coupling for the charged planar black hole in the large mass limit is the same as that obtained due to the Gauss-Bonnet coupling.

## 2 Gauss-Bonnet induced thermal one point function

In this section we will re-visit the set-up of [3] which results in non-trivial thermal one point functions due to the presence of a higher derivative coupling in the low energy effective action. Consider the minimally coupled scalar  $\varphi$  of mass  $m$  in an asymptotically  $AdS_{d+1}$  background. The scalar is dual to an operator  $\mathcal{O}$  of dimensions [14]

$$\Delta = \frac{d}{2} + \sqrt{\frac{d^2}{4} + m^2 R_{\text{AdS}}^2}, \tag{2.1}$$

where  $R_{\text{AdS}}$  is the radius of AdS. If one considers the conventional quadratic action of  $\varphi$ , the symmetry  $\varphi \rightarrow -\varphi$  prevents the dual operator  $\mathcal{O}$  developing an expectation value. In [3], the following the low energy effective action of the scalar was considered

$$S = \frac{1}{16\pi G_N} \int \sqrt{g} d^{d+1}x \left[ \frac{1}{2} (\nabla^\mu \varphi \nabla_\mu \varphi + m^2 \varphi^2) + \alpha \varphi W_{\mu\nu\rho\sigma} W^{\mu\nu\rho\sigma} \right], \tag{2.2}$$

where the scalar  $\varphi$  couples to the Weyl tensor squared. Such couplings are known to be present in the low energy effective action and are dual to the 3-point function involving 2 stress tensors and the operator  $\mathcal{O}$ . Since it is a higher derivative coupling, it is suppressed in the strong t'Hooft coupling limit. From dimensional analysis it is clear that

$$\alpha \sim l_s^2 \sim \frac{R_{\text{AdS}}^2}{\sqrt{\lambda}}, \tag{2.3}$$

where  $l_s$  is the string length and  $\lambda$  is the t' Hooft coupling and the gauge theory. One of the motivations provided in [3] for this choice of the coupling is that the Weyl tensor vanishes for the pure AdS, which is consistent with the one point function of the operator  $\mathcal{O}$  vanishing at zero temperature.

It has been observed that in the study of black hole entropy the Gauss-Bonnet coupling results in the same corrections to black hole entropy as the Weyl tensor squared [15]. Indeed low energy effective actions in string theory contain a coupling of the Gauss-Bonnet term with the dilaton. Motivated by these observations, we will evaluate the expectation value of the one point function by considering the action

$$S = \frac{1}{16\pi G_N} \int \sqrt{g} d^{d+1}x \left[ \frac{1}{2} \left( \nabla^\mu \varphi \nabla_\mu \varphi + m^2 \varphi^2 \right) + \alpha \varphi \mathcal{L}_{\text{GB}} \right], \tag{2.4}$$

where the Gauss-Bonnet term is given by

$$\mathcal{L}_{\text{GB}} = R_{\mu\nu\rho\sigma} R^{\mu\nu\rho\sigma} - 4R_{\mu\nu} R^{\mu\nu} + R^2. \tag{2.5}$$

We will show that the result for the one point function is identical to that obtained by [3]. Though the Gauss-Bonnet curvature for pure AdS is non-vanishing, the one point function evaluated using the coupling in (2.4) does vanish for the pure AdS. Therefore the result is consistent with the vanishing of thermal expectation values at zero temperature.

Using the rules of *AdS/CFT*, the one-point function is given by

$$\langle \mathcal{O}(t, \vec{x}) \rangle = \alpha \int dz' dt' d\vec{x}' \sqrt{g} \tilde{K}(t, \vec{x}; z', t', \vec{x}') \mathcal{L}_{\text{GB}}(z', t', \vec{x}'), \tag{2.6}$$

where  $d\vec{x}' = (dx)^{d-1}$  and  $\tilde{K}(t, \vec{x}; z', t', \vec{x}')$  is the bulk-boundary propagator. The integral over  $t', \vec{x}'$  is carried over the  $AdS_{d+1}$  Schwarzschild black hole. More specifically, the range of integration for the  $t', x'$  coordinates runs from  $-\infty$  to  $\infty$  and the integral over  $z'$  runs from the horizon to infinity. The metric of the planar Schwarzschild black hole is given by

$$ds^2 = \frac{R^2}{z^2} \left( -f(z) dt^2 + \frac{dz^2}{f(z)} + d\vec{x}^2 \right), \quad f(z) = 1 - \frac{z^d}{z_0^d}, \quad z_0 = \frac{\beta d}{4\pi}. \tag{2.7}$$

Here  $R$  is the radius of  $AdS_{d+1}$ ,<sup>2</sup> and  $\beta$  is the inverse temperature. The Gauss-Bonnet curvature of the geometry in (2.7) is given by

$$\mathcal{L}_{\text{GB}}(z) = d(d-2)(d-1)^2 \frac{z^{2d}}{z_0^{2d} R^4} + \frac{(d-2)(d-1)d(d+1)}{R^4}. \tag{2.8}$$

---

<sup>2</sup>From this point onwards  $R$  will refer to the radius of AdS.

It is also useful to evaluate the Weyl tensor squared

$$W_{\mu\nu\rho\sigma}W^{\mu\nu\rho\sigma}(z) = d(d-2)(d-1)^2 \frac{z^{2d}}{z_0^{2d}R^4}. \quad (2.9)$$

Thus the Gauss-Bonnet term and the Weyl tensor squared term differs by a constant. We will see that this additional constant in (2.8) does not contribute to the one point function.

We follow the strategy of [3] to obtain the bulk-boundary propagator. We first solve for the bulk-bulk Greens function in the geometry (2.7) by solving the equation

$$\frac{1}{\sqrt{-g}}\partial_\mu(\sqrt{-g}g^{\mu\nu}\partial_\nu G(z, z', t, t', x, x')) - m^2 G(z, z', t, t', x, x') = \frac{\delta(z-z')\delta(t-t')\delta^{d-1}(\vec{x}-\vec{x}')}{\sqrt{-g}}. \quad (2.10)$$

Then the bulk-boundary propagator can be obtained by [16, 17]

$$K(z', t, t', x, x') = \lim_{z \rightarrow 0} \frac{2\nu}{z^\Delta} G(z, z', t, t', x, x'). \quad (2.11)$$

Since the geometry in (2.7) has translation invariance in  $t, \vec{x}$  directions, we can expand the Greens function in terms of the Fourier modes in these directions<sup>3</sup>

$$G(z, z', t, t', x, x') = \int \frac{d\omega d\vec{k}}{(2\pi)^d} e^{i\omega(t-t') - \vec{k}\cdot(\vec{x}-\vec{x}')} \hat{G}(z, z', \omega, \vec{k}). \quad (2.12)$$

The differential equation obeyed by the Fourier coefficient is given by

$$\begin{aligned} \partial_z \left( \frac{R^{d-1}}{z^{d-1}} f(z) \partial_z \hat{G}(z, z', \omega, \vec{k}) \right) - \frac{R^{d+1}}{z^{d+1}} m^2 \hat{G}(z, z', \omega, \vec{k}) \\ + \frac{R^{d-1}}{z^{d-1}} \left( \frac{\omega^2}{f(z)} - \vec{k}^2 \right) \hat{G}(z, z', \omega, \vec{k}) = \delta(z - z'). \end{aligned} \quad (2.13)$$

Therefore the bulk-boundary propagator also admits the expansion

$$K(z', t, t', x, x') = \int \frac{d\omega d\vec{k}}{(2\pi)^d} e^{i\omega(t-t') - \vec{k}\cdot(\vec{x}-\vec{x}')} \hat{K}(z', \omega, \vec{k}). \quad (2.14)$$

This expansion can then be used in (2.6) to obtain Fourier components of the expectation value, which can be written as

$$\langle \mathcal{O} \rangle_{\omega, \vec{k}} = \int \sqrt{-g} dz' dt' dx' \hat{K}(z', \omega, \vec{k}) e^{-i(\omega t' - \vec{k}\cdot\vec{x}')} \mathcal{L}_{GB}(z', t', \vec{x}'). \quad (2.15)$$

From (2.8) we see that the Gauss-Bonnet curvature only depends on the  $z$  coordinate, This allows us to perform the  $t', x'$  integral to obtain

$$\langle \mathcal{O} \rangle_{\omega, \vec{k}} = (2\pi)^d \delta(\omega) \delta(\vec{k}) \int dz' K(z', 0, 0) \mathcal{L}_{GB}(z'). \quad (2.16)$$

---

<sup>3</sup>For the Euclidean black hole  $t$  is periodic, therefore the Fourier modes in this direction are discrete, this is understood in the paper. For convenience we will denote the sum over these modes by the integral over  $\omega$ .

Thus the only non-zero Fourier coefficient of the expectation value is its zero mode. This implies that the thermal one point functions  $\langle \mathcal{O}(t, \vec{x}) \rangle$  is uniform, independent of time and position. It is convenient to define the zero mode of the bulk-boundary Green's function by

$$\hat{K}(z') = \hat{K}(z', 0, 0) . \tag{2.17}$$

From (2.11) we see that

$$\hat{K}(z') = \lim_{z \rightarrow 0} \frac{2\nu}{z^\Delta} \hat{G}(z, z'), \quad \text{where,} \quad \hat{G}(z, z') = \hat{G}(z, z', \omega, \vec{k})|_{\omega=\vec{k}=0} , \tag{2.18}$$

and  $\hat{G}(z, z')$  satisfies the differential equation

$$\partial_z \left( \frac{R^{d-1}}{z^{d-1}} f(z) \partial_z G(z, z') \right) - \frac{R^{d+1}}{z^{d+1}} m^2 G(z, z') = \delta(z - z') . \tag{2.19}$$

Finally the uniform value of the thermal expectation value is given by

$$\langle \mathcal{O} \rangle = \alpha R^{d+1} \int_0^{z_0} \frac{dz}{z^{(d+1)}} K(z) \mathcal{L}_{\text{GB}}(z) . \tag{2.20}$$

Though this result is obvious because of the translational invariance of the geometry (2.7), we have gone through the steps in detail so that we can generalise this discussion when we consider hyperbolic black holes in section 4.

The Green's function  $G(z, z')$  has to be regular both at  $z = 0$  and at  $z = 1$ . The details of evaluation of this Greens function is given in the appendix A. Let

$$w = \left( \frac{z}{z_0} \right)^d , \quad h = \frac{\Delta}{d} , \tag{2.21}$$

then

$$G(w, w') = -\frac{\Gamma(h)^2}{\Gamma(2h)} \frac{z_0^d}{R^{d-1}d} \left( \varphi_{\text{inf}}(w) \varphi_{\text{hor}}(w') \theta(w' - w) + \varphi_{\text{hor}}(w) \varphi_{\text{inf}}(w') \theta(w - w') \right),$$

$$\varphi_{\text{inf}}(w) = w^h {}_2F_1(h, h, 2h, w), \quad \varphi_{\text{hor}}(w) = w^h {}_2F_1(h, h, 1, 1 - w) . \tag{2.22}$$

Since the hypergeometric function admits a taylor series expansion around the origin, we see that  $\varphi_{\text{inf}}(w)$  is well behaved at infinity  $w = 0$ , while  $\varphi_{\text{hor}}$  is well behaved at the horizon  $w = 1$ . We can now use (2.18) to obtain the bulk to boundary Greens function

$$K(w) = -\frac{\Gamma(h)^2}{\Gamma(2h)} \frac{z_0^d}{R^{d-1}d} \left( \frac{2\nu}{z_0^{\Delta+}} \right) w^h {}_2F_1(h, h, 1, 1 - w) . \tag{2.23}$$

Substituting this in the expression for the one point function in (2.20) we obtain

$$\begin{aligned} \langle \mathcal{O} \rangle &= -\alpha \frac{2\nu}{dz_0^\Delta R^2} \frac{\Gamma(h)^2}{\Gamma(2h)} \int_0^1 dw \left[ (d-2)(d-1)^2 w^h {}_2F_1(h, h, 1, 1 - w) \right. \\ &\quad \left. + (d-2)(d-1)(d+1) w^{h-2} {}_2F_1(h, h, 1, 1 - w) \right] , \\ &= \alpha \frac{(d-2)(d-1)^2}{R^2 d} \frac{\Gamma(h)^2}{\Gamma(2h)} \left( \frac{2\nu}{z_0^{\Delta+}} \right) h(h-1) \pi \csc(h\pi) . \end{aligned} \tag{2.24}$$

Here the second term in the integrand arising from the constant term in the Gauss-Bonnet curvature given in (2.8). To obtain the last line we have used the result

$$\int_0^1 {}_2F_1(h, h; 1; w)(1-w)^{h+n} dw = \frac{\Gamma(-h+n+2)\Gamma(h+n+1)}{\Gamma(n+2)^2} \quad (2.25)$$

if  $\text{Re}(h-n) < 2$  and  $\text{Re}(h+n) > -1$ .

Note that the integral vanishes for  $n = -2$ , therefore the constant contribution of the Gauss-Bonnet curvature vanishes. This ensures the result for the one point function from the Gauss-Bonnet coupling is identical to that of the Weyl tensor squared coupling.

Having obtained the one point in (2.24), to extract the time to singularity, we take the large  $h$  limit with  $h \rightarrow \infty - i\epsilon$ , this results in

$$\begin{aligned} \lim_{h \rightarrow \infty - i\epsilon} \langle \mathcal{O} \rangle &\sim e^{-i\pi h} 2^{-2h}, \\ &= e^{-i\pi \frac{mR}{d}} 4^{-\frac{mR}{d}}. \end{aligned} \quad (2.26)$$

Here we have ignored all the polynomial terms in  $h$  and retained only terms which are exponential in  $h$ . We use the fact that  $\text{Im } h < 0$  to pick up the negative phase, but we can very well pick up the positive phase when  $\text{Im } h > 0$ .

**Comparison with geometric lengths.** Maldacena and Grinberg [3], identified the exponential terms occurring in the expectation value of the one point function with the following geometric lengths associated with the black hole. Consider a radially infalling geodesic with zero energy released at  $z = z_0$ , the horizon. The proper time, the particle takes to reach the singularity  $z = \infty$  is given by the integral

$$\begin{aligned} t_s &= \int_{z_0}^{\infty} \frac{Rdz}{z\sqrt{\left(\frac{z}{z_0}\right)^d - 1}}, \\ &= \frac{\pi R}{d}. \end{aligned} \quad (2.27)$$

Similarly, the regularized space like length from infinity to the horizon is given by

$$\begin{aligned} \hat{\ell}_{\text{hor}} &= \lim_{\epsilon \rightarrow 0} \int_{\epsilon}^{z_0} \frac{Rdz}{z\sqrt{1 - \left(\frac{z}{z_0}\right)^d}}, \\ &= \frac{R}{d} \log 4 - R \log \left(\frac{\epsilon}{z_0}\right) + O(\epsilon). \end{aligned} \quad (2.28)$$

The regularized length is obtained by ignoring the divergence as normalised in [3], which results in

$$\ell_{\text{hor}} = \frac{R}{d} \log 4. \quad (2.29)$$

One point worth mentioning at this stage is that both lengths are independent of the mass of the black hole. The mass unlike these lengths can be obtained easily by studying the behaviour of particles in the black hole geometry. Comparing (2.27) and (2.29), we see



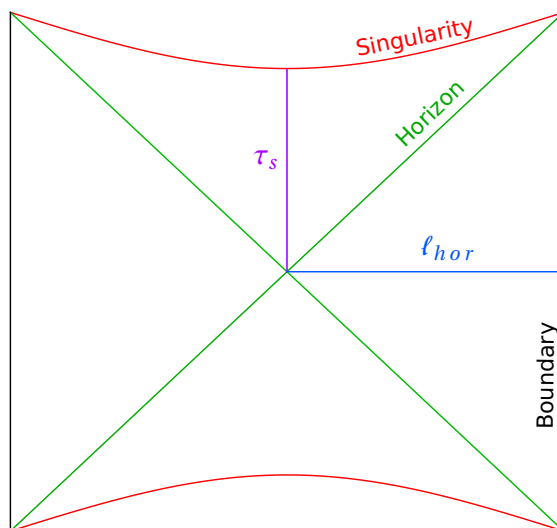


**Figure 1.** Penrose diagram for the AdS-Schwarzschild metric:  $\tau_s$  is the time-like distance between the horizon and the singularity, and  $\ell_{\text{hor}}$  refers to the regularised space-like distance between the boundary and the horizon.

that in the  $h \rightarrow \infty$  limit we can re-write the thermal expectation value in the following geometric form

$$\lim_{m \rightarrow \infty - i\epsilon} \langle \mathcal{O} \rangle \sim \exp(-im\tau_s - m\ell_{\text{hor}}). \quad (2.30)$$

These lengths are shown on the Penrose diagram of the AdS Schwarzschild black hole in figure 1.

### 3 The charged planar black hole at large $d$

Let us consider the planar Reissner-Nördstrom black hole in  $AdS_{d+1}$  whose metric is given by [18].

$$ds^2 = \frac{R^2}{z^2} \left( -f(z)dt^2 + \frac{dz^2}{f(z)} + d\vec{x}^2 \right), \quad f(z) = 1 - \frac{z^d}{z_0^d} + q^2 z^{2d-2}. \quad (3.1)$$

In this section, we wish to evaluate the one point function of the scalar in this background with the action (2.4). Maldacena and Grinberg [3] deal with the case of charged black hole in  $AdS_5$ . Using a saddle point analysis in terms of complex geodesics, they argue that the one point function of the operator dual to a minimally coupled scalar is of the form

$$\langle \mathcal{O} \rangle \sim \exp(-m(\ell_{\text{hor}} + \ell_{\text{sing}} - i\tau_{\text{in}})), \quad (3.2)$$

where  $\ell_{\text{hor}}$  is the regularized distance from the boundary to the outer horizon,  $\ell_{\text{sing}}$  is the distance from the inner horizon to the singularity and finally  $\tau_{\text{in}}$  is the time from the inner horizon to the outer horizon. These lengths are shown in the figure 2. Note that here compared to the case without the inner horizon there is an additional dependence of  $\ell_{\text{sing}}$ .

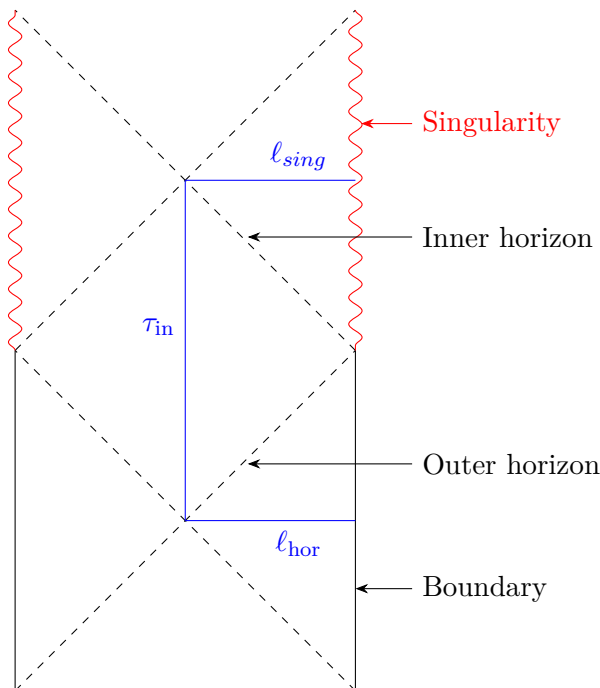


**Figure 2.** The three lengths  $\tau_{\text{in}}, \ell_{\text{hor}}, \ell_{\text{sing}}$  shown on the Penrose diagram of the charged black hole in AdS.

The argument in [3] involved a saddle with a contour that goes over to complex radial positions. It would be more satisfying if the direct analysis similar to that performed in for the Schwarzschild black hole in section 2 can be done for a black hole with inner horizon. In this section we show that indeed it is possible to arrive at an exact expression for the thermal one point function in a suitable large  $d$  limit. Just as in the Schwarzschild case in (2.24), the integral which results in the one point function involves an integral from the outer horizon to infinity.

To begin, let us examine the equation of the minimally coupled scalar (3.1) in the background for the zero mode in the directions along the boundary.

$$(1-w)w^2\varphi''(w) - w^2\phi'(w) - h(h-1)\varphi(w) + \frac{q^2w^{3-\frac{2}{d}}z_0^{2d-2}}{d} (2(d-1)\phi'(w) + wd\varphi''(w)) = 0. \tag{3.3}$$

Here we have used the co-ordinate

$$w = \left(\frac{z}{z_0}\right)^d. \tag{3.4}$$

We will see that  $w$  is always finite in the domain we wish to evaluate the integral involving the one point function. To obtain a more tractable equation, we take the following large  $d$  limit

$$d \rightarrow \infty, \quad \text{with} \quad q^2z_0^{2d-2} = Q, \quad \text{held fixed.} \tag{3.5}$$

In this limit the equation (3.3)<sup>4</sup> reduces to

$$(1-w)w^2\varphi''(w) - w^2\varphi'(w) - h(h-1)\varphi(w) + Qw^3[2\varphi'(w) + w\varphi''(w)] = 0. \quad (3.6)$$

Solutions of this differential equation can be written in terms of hypergeometric functions. Before we go ahead, let us obtain the locations of the horizons in the limit (3.5). The function  $f(z)$  in (3.1) becomes

$$\begin{aligned} f(w) &= 1 - w + Qw^2w^{-\frac{2}{d}}, \\ \hat{f}(w) &= \lim_{d \rightarrow \infty} f(w) = 1 - w + Qw^2. \end{aligned} \quad (3.7)$$

Therefore the inner and the outer horizons are at

$$w_{\text{in}} = \frac{1 + \sqrt{1 - 4Q}}{2Q}, \quad w_{\text{out}} = \frac{1 - \sqrt{1 - 4Q}}{2Q}. \quad (3.8)$$

To construct the Green's function we need the well behaved solutions of (3.6) at infinity and at the horizon. These are given by

$$\begin{aligned} \varphi_{\text{inf}} &= w^h(w - 2 - \sqrt{1 - 4Q}w)^{-h} {}_2F_1\left(h, h, 2h, \frac{2\sqrt{1 - 4Q}w}{2 + (\sqrt{1 - 4Q} - 1)w}\right), \\ \varphi_{\text{hor}} &= w^h(w - 2 - \sqrt{1 - 4Q}w)^{-h} {}_2F_1\left(h, h, 1, 1 - \frac{2\sqrt{1 - 4Q}w}{2 + (\sqrt{1 - 4Q} - 1)w}\right). \end{aligned} \quad (3.9)$$

It is easy to observe that  $\varphi_{\text{inf}}$  is well behaved at the boundary  $w \rightarrow 0$ , while  $\varphi_{\text{hor}}$  is well behaved at the outer horizon  $w_{\text{out}}$ . The Greens function satisfies the equation

$$\partial_w(\hat{f}(w)\partial_w G(z, z')) - \frac{h(h-1)}{w^2} = \frac{z_0^d}{dR^{d-1}}\delta(w - w'). \quad (3.10)$$

Here note that the function  $f(w)$  has been replaced by its limit  $\hat{f}(w)$ . The Green's function is obtained by using the two solutions in (3.9) and is given by

$$\begin{aligned} G(w, w') &= -2^{2h}(1 - 4Q)^{h-\frac{1}{2}} \frac{(\Gamma(h))^2}{\Gamma(2h)} \frac{z_0^d}{R^{d-1}d} \\ &\times \left( \varphi_{\text{inf}}(w)\varphi_{\text{hor}}(w')\theta(w' - w) + \varphi_{\text{hor}}(w)\varphi_{\text{inf}}(w')\theta(w - w') \right). \end{aligned} \quad (3.11)$$

The bulk boundary propagator using (2.18) is given by

$$\begin{aligned} K(w) &= -2^{2h}(1 - 4Q)^{h-\frac{1}{2}} \frac{(\Gamma(h))^2}{\Gamma(2h)} \frac{z_0^d}{R^{d-1}d} (-2)^h \left( \frac{2\nu}{z_0^\Delta} \right) \\ &\times w^h(w - 2 - \sqrt{1 - 4Q}w)^{-h} {}_2F_1\left(h, h, 1, 1 - \frac{2\sqrt{1 - 4Q}w}{2 + (\sqrt{1 - 4Q} - 1)w}\right). \end{aligned} \quad (3.12)$$

---

<sup>4</sup>In appendix B, we discuss how taking the large  $d$  limit as in (3.5), the solution in (3.1) satisfies the leading order Einstein's equation.

Finally, we need the limiting value of the Gauss-Bonnet curvature in the large  $d$  limit. Evaluating the Gauss-Bonnet curvature for the geometry in (3.1), we obtain

$$\begin{aligned} \mathcal{L}_{GB} = & \frac{(d-2)(d-1)}{R^4} \times \\ & \left( (3d-5)(3d-4)Q^2w^{4-\frac{4}{d}} - 2Q[d\{d(4w-1) - 10w + 5\} + 6(w-1)]w^{2-\frac{2}{d}} \right. \\ & \left. + d[(d-1)w^2 + d + 1] \right). \end{aligned} \quad (3.13)$$

Taking the limit  $d \rightarrow \infty$ , the leading contribution to the Gauss Bonnet term is given by

$$\lim_{d \rightarrow \infty} \mathcal{L}_{GB} = \frac{d^4}{R^4} \left( 9Q^2w^4 - 8w^3Q + (2Q+1)w^2 + 1 \right). \quad (3.14)$$

We now have all the necessary ingredients to evaluate the one point function in the large  $d$  limit. Substituting the leading contribution of the Gauss-Bonnet curvature (3.14) and the bulk boundary propagator (3.12) in (2.20), we obtain for the thermal one point function

$$\begin{aligned} \langle \mathcal{O} \rangle = & -\alpha 2^{2h} \frac{d^2(-2)^{-h}(1-4Q)^{h-\frac{1}{2}}}{R^2} \frac{\Gamma(h)^2}{\Gamma(2h)} \left( \frac{2\nu}{z_0^{\Delta_+}} \right) \int_0^{w_{\text{out}}} dw \left[ 9Q^2w^2 - 8wQ + (2Q+1) + \frac{1}{w^2} \right] \\ & \times w^h (w-2-\sqrt{1-4Q}w)^{-h} {}_2F_1(h, h, 1, 1 - \frac{2\sqrt{1-4Q}w}{2+(\sqrt{1-4Q}-1)w}). \end{aligned} \quad (3.15)$$

One simple check of this result is to note that when  $Q \rightarrow 0$ , this expression reduces to the integral obtained in the uncharged planar black hole in (2.24) with  $d \rightarrow \infty$ . Examining (3.14) and (3.15), we see that we need to keep the ratio  $\frac{d}{R}$  to be finite in the large  $d$  limit to ensure these quantities are finite. Note that the integral is from the outer horizon to infinity, therefore in the domain of integration in  $w$  is always finite. We can bring the range of integration from 0 to 1 by making the substitution

$$y = 1 - \frac{2\sqrt{1-4Q}w}{2+(\sqrt{1-4Q}-1)w}, \quad (3.16)$$

The one point function then is given by

$$\begin{aligned} \langle \mathcal{O} \rangle = & \frac{4d^2(1-4Q)^{h/2}}{R^2} \frac{(\Gamma(h))^2}{\Gamma(2h)} \left( \frac{2\nu}{z_0^{\Delta_+}} \right) \int_0^1 dy {}_2F_1(h, h; 1; y) \times \\ & \left[ -\frac{9(1-y)^{h+2}}{4Q^2w_{\text{in}}^4(1-\chi y)^4} + \frac{2(1-y)^{h+1}}{Q^2w_{\text{in}}^3(1-\chi y)^3} - \frac{(2Q+1)(1-y)^h}{4Q^2w_{\text{in}}^2(1-\chi y)^2} - \frac{(1-y)^{h-2}}{4} \right], \end{aligned} \quad (3.17)$$

where

$$\chi = \frac{1-\sqrt{1-4Q}}{1+\sqrt{1-4Q}}. \quad (3.18)$$

The integral of the first three terms in the square bracket in (3.17) can be done using formula (7.512.9) in [19].<sup>5</sup> From (2.25), we can see that integral of the last term in the

---

<sup>5</sup>  $\int_0^1 dx x^{\gamma-1}(1-x)^{\rho-1}(1-\chi x)^{-\sigma} {}_2F_1(\alpha, \beta, \gamma, x) = \frac{(1-\chi)^{-\sigma} \Gamma(\gamma)\Gamma(\rho)\Gamma(-\alpha-\beta+\gamma+\rho)}{\Gamma(-\alpha+\gamma+\rho)\Gamma(-\beta+\gamma+\rho)} \times {}_3F_2\left(\rho, \sigma, -\alpha-\beta+\gamma+\rho; -\alpha+\gamma+\rho, -\beta+\gamma+\rho; \frac{\chi}{\chi-1}\right).$

square bracket vanishes. Using the result for the integrals we obtain

$$\begin{aligned}
 \langle \mathcal{O} \rangle = & -\frac{d^2(1-4Q)^{\frac{h}{2}-1}}{2R^2(1-\sqrt{1-4Q})} \frac{(\Gamma(h))^2}{\Gamma(2h)} \left(\frac{2\nu}{z_0^\Delta}\right) \pi(h-1)h \csc(\pi h) \times \\
 & \left\{ \left[ (-3h^2 - h + 10)Q + \sqrt{1-4Q} \left( (3h^2 - 3h - 2)Q + 2 \right) - 2 \right] \times \right. \\
 & {}_2F_1\left(2-h, h+1; 2; \frac{1}{2} - \frac{1}{2\sqrt{1-4Q}}\right) \\
 & \left. + 4Q(h-2) {}_2F_1\left(3-h, h+1; 2; \frac{1}{2} - \frac{1}{2\sqrt{1-4Q}}\right) \right\}. \tag{3.19}
 \end{aligned}$$

Here the  ${}_3F_2$  hypergeometric function simplifies to  ${}_2F_1$  for the values of the parameters resulting from the integral.

Having obtained the leading contribution to the one point function in the large  $d$  limit we can analytically continue  $h$  and take the large  $h$  limit. Note that

$$h = \frac{\Delta}{d}. \tag{3.20}$$

As we are taking the large  $d$  limit, we would need to ensure that  $\Delta$  grows faster than linear in  $d$  so that  $h$  remains large.  $h$  occurs as a parameter of the hypergeometric functions in (3.19), therefore we need the asymptotic expansion for large orders. To proceed, we first write down the asymptotic expansion obtained by Watson [20], for hypergeometric functions at large orders

$$\begin{aligned}
 & {}_2F_1\left(\alpha + \lambda, \beta - \lambda, \gamma; \frac{1}{2} - \frac{z}{2}\right) \\
 & \sim \frac{\Gamma(1 - \beta + \lambda)\Gamma(\gamma)}{\pi\Gamma(\gamma - \beta + \lambda)} 2^{\alpha+\beta-1} (1 - e^{-\zeta})^{\frac{1}{2}-\gamma} (1 + e^{-\zeta})^{\gamma-\alpha-\beta-\frac{1}{2}} \\
 & \times \sum_{s=0}^{\infty} \left[ c_s e^{(\lambda-\beta)\zeta} \Gamma\left(s + \frac{1}{2}\right) \lambda^{-s-\frac{1}{2}} + c'_s e^{\mp\pi i(\frac{1}{2}-\gamma)} e^{-(\lambda+\alpha)\zeta} \Gamma\left(s + \frac{1}{2}\right) \lambda^{-s-\frac{1}{2}} \right]. \tag{3.21}
 \end{aligned}$$

This expansion is valid for large  $|\lambda|$  with  $\alpha, \beta, z$  fixed, the constants  $c_s$  can be found in [20]. Here

$$\zeta = \text{arcCosh } z \tag{3.22}$$

For our purpose it is sufficient to obtain, the leading term in this expansion. So we can retain the first term with  $s = 0$ . All other terms are sub-leading, they are either exponentially or polynomially suppressed in  $\lambda$ . Therefore we have

$$\begin{aligned}
 & {}_2F_1\left(\alpha + \lambda, \beta - \lambda, \gamma; \frac{1}{2} - \frac{z}{2}\right) \\
 & \sim \frac{\Gamma(1 - \beta + \lambda)\Gamma(\gamma)}{\pi\Gamma(\gamma - \beta + \lambda)} 2^{\alpha+\beta-1} (1 - e^{-\zeta})^{\frac{1}{2}-\gamma} (1 + e^{-\zeta})^{\gamma-\alpha-\beta-\frac{1}{2}} e^{(\lambda-\beta)\zeta} \Gamma\left(\frac{1}{2}\right) \lambda^{-\frac{1}{2}}, \tag{3.23}
 \end{aligned}$$

with  $c_0 = 1$  as given in [20]. Substituting the arguments of the hypergeometric function that we have in (3.19), we obtain the following leading contributions

$$\begin{aligned} \lim_{h \rightarrow \infty} {}_2F_1 \left( 2 - h, 1 + h, 2, \frac{1}{2} - \frac{1}{2\sqrt{1-4Q}} \right) &\sim \frac{e^{h \operatorname{arcsech}(\sqrt{1-4Q})}}{h^{3/2}}, \\ \lim_{h \rightarrow \infty} {}_2F_1 \left( 3 - h, 1 + h, 2, \frac{1}{2} - \frac{1}{2\sqrt{1-4Q}} \right) &\sim \frac{e^{h \operatorname{arcsech}(\sqrt{1-4Q})}}{h^{3/2}}. \end{aligned} \quad (3.24)$$

Finally we can substitute the asymptotic form in (3.24) and take the large  $h$  limit in the rest of the terms in the thermal one point function given in (3.19) which results in

$$\lim_{h \rightarrow \infty - i\epsilon} \langle \mathcal{O} \rangle \sim e^{-h \log \left[ \frac{4}{\sqrt{1-4Q}} \right] + h \operatorname{arcsech}(\sqrt{1-4Q})} e^{-i\pi h} [1 + e^{-i2\pi h} + \dots] \times (\text{powers of } h). \quad (3.25)$$

Here we have followed the prescription in [3] and given a small imaginary part to  $h$  so as to pick up the phase  $e^{-i\pi h}$ . Now replacing  $h$  by the mass in the large  $h$  or mass limit we obtain

$$\langle \mathcal{O} \rangle \sim \exp \left[ m \left( -\frac{R}{d} \log \left[ \frac{4}{\sqrt{1-4Q}} \right] + \frac{R}{d} \operatorname{arcsech}(\sqrt{1-4Q}) - i\pi \frac{R}{d} \right) \right]. \quad (3.26)$$

**Comparison with geometric lengths.** Let us now evaluate the lengths  $\tau_s, \ell_{\text{hor}}, \ell_{\text{sing}}$ . The proper time between the outer and inner horizons is given by

$$\tau_s = \int_{z_{\text{in}}}^{z_{\text{out}}} \frac{R dz}{z \sqrt{\frac{z^d}{z_0^d} - qz^{2d-2} - 1}}. \quad (3.27)$$

We re-write this integral in terms of  $w$  defined in (3.4) and take the large  $d$  limit of (3.5) to obtain

$$\begin{aligned} \tau_s &= \frac{R}{d\sqrt{Q}} \int_{w_{\text{out}}}^{w_{\text{in}}} \frac{dw}{w \sqrt{(w - w_{\text{out}})(w_{\text{in}} - w)}}, \\ &= \frac{\pi R}{d}. \end{aligned} \quad (3.28)$$

The proper length from the outer horizon to infinity is given by

$$\begin{aligned} \hat{\ell}_{\text{hor}} &= \lim_{\epsilon \rightarrow 0} \frac{R}{d\sqrt{Q}} \int_{\left(\frac{\epsilon}{z_0}\right)^d}^{w_{\text{out}}} \frac{dw}{w \sqrt{(w_{\text{out}} - w)(w_{\text{in}} - w)}}, \\ &= \frac{R}{d} \log \left( \frac{4}{\sqrt{1-4Q}} \right) - R \log \left( \frac{\epsilon}{z_0} \right). \end{aligned} \quad (3.29)$$

Again the regularised length is obtained by ignoring the divergence, note that from (2.29), we see that the divergence is identical to that for the planar Schwarzschild black hole.

$$\ell_{\text{hor}} = \frac{R}{d} \log \left( \frac{4}{\sqrt{1-4Q}} \right). \quad (3.30)$$

The proper length from the inner horizon to the singularity is given by

$$\begin{aligned} \ell_{\text{sing}} &= \frac{R}{d\sqrt{Q}} \int_{w_{\text{in}}}^{\infty} \frac{dw}{w\sqrt{(w_{\text{out}} - w)(w_{\text{in}} - w)}}, \\ &= \frac{R}{d} \operatorname{arcsech}(\sqrt{1 - 4Q}). \end{aligned} \tag{3.31}$$

We use these geometric lengths to rewrite the one point function obtained in (3.26) in the following form

$$\langle \mathcal{O} \rangle \sim \exp(-m(\ell_{\text{hor}} + \ell_{\text{sing}} - i\tau_s)). \tag{3.32}$$

This is the generic structure of the one point function which was argued using a saddle point approach in [3]. This involved a choice of contour in the complex radial coordinate. Here we have obtained it by explicitly evaluating the one point function which involves an integral from the outer horizon to infinity exactly at large  $d$ . The one point function contains the information of the inner horizon. In the appendix C, we show that the same structure of the one point function is obtained for the Weyl tensor squared coupling.

## 4 Hyperbolic black holes

In this section, we consider the hyperbolic black hole in  $AdS_{d+1}$  [21, 22] whose metric is given by

$$ds^2 = \frac{R^2}{z^2} \left[ - \left( 1 - \frac{z^2}{R^2} \right) dt^2 + \frac{dz^2}{1 - \frac{z^2}{R^2}} + R^2 (du^2 + \sinh^2 u d\Omega_{d-2}^2) \right], \tag{4.1}$$

where  $R$  is the radius of  $AdS_{d+1}$  and  $\Omega_{d-2}$  refers to the sphere  $S^{d-2}$ . The coordinate  $z$  is related to the usual radial co-ordinate by  $z = \frac{R^2}{r}$ . This metric can be obtained from a hyperbolic slicing of pure  $AdS_{d+1}$  and can be interpreted as a black hole with a horizon at  $z = R$  with Hawking temperature

$$T = \frac{1}{2\pi R}. \tag{4.2}$$

This space is holographically dual to a conformal field theory on  $R \times AdS_d$  [23, 24]. We would like to repeat the analysis done in the previous sections for this background and check if indeed the one point function contains information of the time from the horizon to singularity.

We consider the effective action in (2.4) with Gauss-Bonnet coupling. The Gauss-Bonnet coupling in this case is a constant which is given by

$$\mathcal{L}_{GB} = \frac{c}{R^4}, \quad c = (d-2)(d-1)d(d+1). \tag{4.3}$$

To construct the bulk-boundary propagator, we follow the procedure discussed in section. Since the spatial geometry of the boundary is Euclidean  $AdS_{d-1}$ , we need to expand the bulk-bulk Green's function in terms of normalizable eigen functions on  $AdS_{d-1}$ . We consider the expansion

$$G(z, z', t, t', u, u', \Omega, \Omega') = \int d\omega d\lambda \sum_{l, \sigma} \hat{G}(z, z', \lambda, l, \sigma) \phi_{l\sigma}(u, \Omega) \phi_{l\sigma}^*(u', \Omega') e^{-i\omega(t-t')}, \tag{4.4}$$

where  $\phi_{\lambda\sigma}$  are eigen functions of the Laplacian on Euclidean  $AdS_{d-1}$ . They satisfy the equation

$$\square\phi_{\lambda\sigma} = -\left(\lambda^2 + \left(\frac{d-2}{2}\right)^2\right)\phi_{\lambda\sigma}, \quad (4.5)$$

and the quantum number  $\lambda$  is a continuous variable that runs from 0 to  $\infty$ . The numbers  $(l, \sigma)$  refer to quantum numbers on  $\Omega_{d-2}$  and  $l$  is an integer that runs from 0 to  $\infty$ ,  $\sigma$  refer to the other quantum numbers of the spherical harmonics. These eigen functions have been explicitly constructed in [25] and they are given by

$$\begin{aligned} \phi_{\lambda\sigma} &= q_{\lambda,l}(u)Y_{l\sigma}(\Omega), \\ q_{\lambda,l}(u) &= (i \sinh u)^l {}_2F_1\left(i\lambda + \frac{d-2}{2} + l, -i\lambda + \frac{d-2}{2} + l, l + \frac{d-1}{2}; -\sinh^2 \frac{u}{2}\right). \end{aligned} \quad (4.6)$$

What is important for us is their orthonormality property on  $AdS_{d-1}$

$$\int dud\Omega_{d-2}(\sinh u)^{d-2} \phi_{\lambda\sigma}(u, \Omega)\phi_{\lambda'\sigma'}(u, \Omega) = \delta_{l,l'}\delta_{\sigma,\sigma'}\delta(\lambda - \lambda'), \quad (4.7)$$

where the integral is on  $AdS_{d-1}$  with unit radius. Substituting the expansion of the Green's function given in (4.4) and using the metric (4.1) we see that the coefficients obey the differential equation

$$\begin{aligned} \partial_z \left( \left(\frac{R}{z}\right)^{d-1} \left(1 - \frac{z^2}{R^2}\right) \partial_z \hat{G}(z, z', \omega, \lambda, l, \sigma) \right) + \left(\frac{R}{z}\right)^{d-1} \frac{\omega^2}{1 - \frac{z^2}{R^2}} \hat{G}(z, z', \omega, \lambda, l, \sigma) \\ - \left(\frac{R}{z}\right)^{d-1} \left[ m^2 \left(\frac{R}{z}\right)^2 + \frac{1}{R^2} \left(\lambda^2 + \left(\frac{d-2}{2}\right)^2\right) \right] \hat{G}(z, z', \omega, \lambda, l, \sigma) \\ = \frac{1}{R^{d-1}} \delta(z - z'). \end{aligned} \quad (4.8)$$

Similarly the bulk-boundary Green's function admits an eigenfunction expansion given by

$$K(z', t, t' u, u', \Omega, \Omega') = \int d\omega d\lambda \sum_{l,\sigma} \hat{K}(z', \omega, \lambda, l, \sigma) \phi_{\lambda\sigma}(u, \Omega) \phi_{\lambda\sigma}^*(u', \Omega') e^{-i\omega(t-t')}. \quad (4.9)$$

From (2.11) and the eigen function expansions we see that

$$\hat{K}(z', \omega, \lambda, l, \sigma) = \lim_{z \rightarrow 0} \frac{2\nu}{z^\Delta} \hat{G}(z, z', \omega, \lambda, l, \sigma). \quad (4.10)$$

Then substituting the eigenmode expansion in the expression for thermal one point function given in (2.6), we can obtain the expectation value of each mode

$$\langle \mathcal{O} \rangle_{w,\lambda,l,\sigma} = \alpha \int dz' dt' du' d\Omega' \sqrt{g'} \hat{K}(z', \omega, \lambda, l, \sigma) e^{i\omega t'} \phi_{\lambda\sigma}^*(u', \Omega') \mathcal{L}_{GB}(z', t', u', \Omega'), \quad (4.11)$$

where the metric is that given in (4.1). From (4.3), we see that the Gauss-Bonnet term is independent of time or coordinates on  $AdS_{d-1}$ . This implies that we can perform the  $t$  integral, furthermore since the bulk-boundary propagator is independent of the quantum



numbers  $l, \sigma$  due to spherical symmetry we can perform the integral on the sphere  $S^{d-2}$ . This leads to

$$\langle \mathcal{O} \rangle_{w,\lambda,l,\sigma} = \alpha 2\pi \delta(w) \delta_{l,0} \delta_{\sigma,0} \int dz \frac{R^{2d}}{z^{d+1}} \hat{K}(z, 0, \lambda, 0, 0) \mathcal{L}_{GB}(z) \int du (\sinh u)^{d-2} q_{\lambda,0}^*(u). \quad (4.12)$$

The integral over  $u$  needs to be regulated by placing a cut off in the coordinate  $u$  which is along the field theory directions. This will yield a function which just depends on the mode  $\lambda$  it does not contain the information of the operator  $\mathcal{O}$ . Therefore, let us define the thermal one point function of the mode  $\lambda$ , by scaling out the integral over  $u$ .

$$\begin{aligned} \langle \hat{\mathcal{O}} \rangle_\lambda &= \alpha \int dz \frac{R^{2d}}{z^{d+1}} \hat{K}(z, \lambda) \mathcal{L}_{GB}(z), \\ \hat{K}(z, \lambda) &= \hat{K}(z, 0, \lambda, 0, 0). \end{aligned} \quad (4.13)$$

Here it is understood we are in the zero mode sector  $\omega = 0, l = 0, \sigma = 0$ . It is easy to see that in case the rescaled expectation value  $\langle \hat{\mathcal{O}} \rangle_\lambda$  is independent of  $\lambda$ , then it implies that the thermal one point function  $\langle \mathcal{O}(t, u, \Omega) \rangle$  is uniform in the field theory directions. This is because if  $\langle \mathcal{O}(t, u, \Omega) \rangle$  is constant on  $R \times AdS_{d-1}$ , then each mode expansion of the expectation value is given by

$$\begin{aligned} \langle \mathcal{O} \rangle_{w,\lambda,l,\sigma} &= \int dt du d\Omega_{d-2} (\sinh u)^{d-2} \langle \mathcal{O}(t, u, \Omega) \rangle e^{i\omega t} q_{\lambda,l}^*(u) Y_{l\sigma}^*(\Omega), \\ &= \langle \mathcal{O} \rangle 2\pi \delta(w) \delta_{l,0} \delta_{\sigma,0} R^{d-1} \int du (\sinh u)^{d-2} q_{\lambda,0}^*. \end{aligned} \quad (4.14)$$

In the second line we have used the fact that  $\langle \mathcal{O}(t, u, \Omega) \rangle$  is constant on  $R \times AdS_{d-1}$ . Comparison of (4.12), (4.13) and the second line of (4.14) shows that in case  $\langle \hat{\mathcal{O}} \rangle_\lambda$  is independent of  $\lambda$ , then it can be identified with the uniform expectation value of the operator in the field theory. Therefore we will evaluate the thermal expectation value given in (4.13) and show that in the regime of our interest, that is large operator dimensions  $\Delta$ , the expectation value is independent of  $\lambda$  and it coincides with the uniform expectation value on the boundary field theory on the hyperbolic space.

To obtain the Green's function  $\hat{G}(z, z', 0, \lambda, 0, 0) \equiv \hat{G}(z, z', \lambda)$ , it is convenient to go to coordinates

$$w = \frac{z^2}{R^2}. \quad (4.15)$$

Then the equation (4.8) is written as

$$\begin{aligned} &4\partial_w \left[ w^{(1-\frac{d}{2})} (1-w) \partial_w \hat{G}(w, w', \lambda) \right] \\ &- w^{-(1+\frac{d}{2})} \left[ m^2 R^2 + w \left( \lambda^2 + \left( \frac{d-2}{2} \right)^2 \right) \right] \hat{G}(w, w', \lambda) = \frac{2}{R^{d-2}} \delta(w-w'). \end{aligned} \quad (4.16)$$

The Green's function is constructed by using the solution to the homogenous equation The solution which is regular at the boundary  $z = 0$  is given by

$$\varphi_{\text{inf}}(w) = w^{\Delta/2} {}_2F_1 \left( -\frac{d}{4} + \frac{\Delta}{2} - \frac{i\lambda}{2} + \frac{1}{2}, -\frac{d}{4} + \frac{\Delta}{2} + \frac{i\lambda}{2} + \frac{1}{2}; -\frac{d}{2} + \Delta + 1; w \right), \quad (4.17)$$

while the solution regular at the horizon is given by

$$\varphi_{\text{hor}}(w) = w^{\Delta/2} {}_2F_1\left(-\frac{d}{4} + \frac{\Delta}{2} - \frac{i\lambda}{2} + \frac{1}{2}, -\frac{d}{4} + \frac{\Delta}{2} + \frac{i\lambda}{2} + \frac{1}{2}; 1; 1-w\right). \quad (4.18)$$

Then the Greens function which solves (4.16) is obtained by the same methods discussed in the appendix A. This results in

$$\begin{aligned} \hat{G}(w, w', \lambda) &= A \times \left( \varphi_{\text{inf}}(w) \varphi_{\text{hor}}(w') \theta(w' - w) + \varphi_{\text{hor}}(w) \varphi_{\text{inf}}(w') \theta(w - w') \right), \quad (4.19) \\ A &= -\frac{R^{2-d} \Gamma\left(\frac{d}{2} - \Delta\right) \Gamma\left(\frac{1}{4}(-d + 2\Delta - 2i\lambda + 2)\right) \Gamma\left(\frac{1}{4}(-d + 2\Delta + 2i\lambda + 2)\right)}{2\Gamma\left(\frac{1}{2}(d - 2\Delta)\right) \Gamma\left(\frac{1}{2}(2\Delta - d) + 1\right)}. \end{aligned}$$

The bulk-boundary Greens' function can be read out using (4.10)

$$\hat{K}(w, \lambda) = \frac{2\nu}{R^\Delta} A \varphi_{\text{hor}}(w). \quad (4.20)$$

Substituting this in the expression for the thermal one point function in (4.13), we obtain

$$\langle \hat{\mathcal{O}} \rangle_\lambda = \alpha \frac{2\nu}{R^\Delta} \frac{c}{2R^4} A R^d \int_0^1 dw w^{-(\frac{d}{2}+1)} \varphi_{\text{hor}}(w). \quad (4.21)$$

We change variables from  $w$  to  $1-w$  to re-write the integral as

$$\begin{aligned} \langle \hat{\mathcal{O}} \rangle_\lambda &= \alpha \frac{2\nu}{R^\Delta} \frac{c}{2R^4} A R^d \times \quad (4.22) \\ &\int_0^1 dw (1-w)^{-\frac{\Delta}{2}-1} {}_2F_1\left(\frac{1}{4}(d - 2\Delta - 2i\lambda + 2), \frac{1}{4}(d - 2\Delta + 2i\lambda + 2); 1; w\right), \end{aligned}$$

We can perform the integral by using the formula

$$\begin{aligned} \int_0^1 (1-w)^a {}_2F_1(b, c; 1; w) dw &= \frac{\Gamma(a+1)\Gamma(a-b-c+2)}{\Gamma(a-b+2)\Gamma(a-c+2)}, \quad (4.23) \\ &\text{if } \text{Re}(a) > -1 \text{ and } \text{Re}(a) + 2 > \text{Re}(b+c), \end{aligned}$$

which results in

$$\begin{aligned} \langle \hat{\mathcal{O}} \rangle_\lambda &= -\alpha \frac{2\nu}{R^\Delta} \frac{c}{R^2} \times \quad (4.24) \\ &\frac{\Gamma\left(-\frac{\Delta}{2}\right) \Gamma\left(\frac{\Delta-d}{2}\right) \Gamma\left(\frac{1}{4}(-d + 2\Delta - 2i\lambda + 2)\right) \Gamma\left(\frac{1}{4}(-d + 2\Delta + 2i\lambda + 2)\right)}{4\Gamma\left(-\frac{d}{2} + \Delta + 1\right) \Gamma\left(\frac{1}{4}(-d - 2i\lambda + 2)\right) \Gamma\left(\frac{1}{4}(-d + 2i\lambda + 2)\right)}. \end{aligned}$$

Observe the factor  $R^{\Delta+2}$  provides the right scaling dimension for the expectation value.

Now that we have the exact expectation value of the operator, we can take the large  $\Delta \rightarrow \infty - i\epsilon$  limit with  $\lambda$  fixed we obtain

$$\lim_{\Delta \rightarrow \infty - i\epsilon} \langle \hat{\mathcal{O}} \rangle_\lambda \sim \csc\left(\frac{\pi\Delta}{2}\right) e^{-\Delta \log(2)} \times (\text{powers of } \Delta). \quad (4.25)$$

From our earlier discussion, we can conclude that since this value is independent of  $\lambda$ , we can conclude that in the large  $\Delta$  limit the operator acquires uniform expectation value on the field theory directions  $R \times AdS_{d-1}$ . Using  $\Delta \sim mR$  in the large  $\Delta$  limit and ignoring corrections due to powers of  $\Delta$ , we can re-write this uniform thermal expectation value as

$$\lim_{\Delta \rightarrow \infty - i\epsilon} \langle \mathcal{O} \rangle \sim \exp\left[m\left(-\frac{i\pi R}{2} - R \log 2\right)\right]. \quad (4.26)$$

**Comparison with geometric lengths.** At this stage we can compare the form of the thermal expectation value in (4.26) with the expression proposed in [3] in terms of geometric lengths. The proper time from the horizon to singularity for the hyperbolic black hole in (4.1) is given by

$$\tau_s = R \int_R^\infty \frac{dz}{z\sqrt{\frac{z^2}{R^2} - 1}} = \frac{\pi R}{2}. \tag{4.27}$$

Recall that the radial co-ordinate  $r = \frac{R^2}{z}$ . Note that unlike the planar Schwarzschild black hole, this length is independent of the dimension  $d$ . The proper length from infinity to the horizon is given by

$$\begin{aligned} \hat{\ell}_{\text{hor}} &= \lim_{\epsilon \rightarrow 0} R \int_\epsilon^R \frac{dz}{z\sqrt{1 - \frac{z^2}{R^2}}}, \\ &= R \log(2) - R \log\left(\frac{\epsilon}{R}\right). \end{aligned} \tag{4.28}$$

The regularized proper length is obtained by ignoring the divergence, so we obtain

$$\ell_{\text{hor}} = R \log(2). \tag{4.29}$$

Using the proper time and the regularized proper length, we can write the expectation value in (4.26) as

$$\lim_{m \rightarrow \infty - i\epsilon} \langle \mathcal{O} \rangle \sim \exp(-im\tau_s - m\ell_{\text{hor}}). \tag{4.30}$$

Therefore we see that the geometric form for the expectation value for operators of large dimensions is true even in the presence of black holes with hyperbolic horizons. One of the consequences of our calculation is that generically, we expect operators of large dimensions on conformal field theories on spatial hyperbolic surfaces to obtain expectation values at finite temperature.

## 5 BTZ black holes with angular momentum

In [3], the examples considered did not include the rotating black holes, moreover it is not clear that the saddle point arguments to arrive at the thermal expectation value provided in [3] for black holes with inner horizons generalise to that of black holes with rotation. This is because these metrics which was used in the saddle point arguments had spherical symmetry. In this section we use the rotating BTZ black hole geometry to study the behaviour of thermal one point function of scalars dual to primaries in the CFT. Though many quantities are exactly solvable in this geometry, one apparent difficulty with this is that in the dual field theory conformal invariance in  $2d$  ensures that primary operators do not acquire non-trivial expectation values at finite temperature if the CFT is on a real line. In the 3 dimensional dual holographic description, this is reflected in the fact that both the Gauss-Bonnet curvature as well Weyl tensor curvature square vanishes in  $3d$ . Therefore the mechanism discussed in the previous sections does not apply to holographic  $2d$  CFTs.

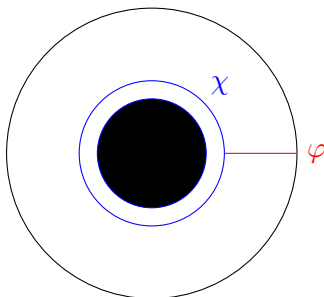


**Figure 3.** One point function induced by the cubic coupling  $\chi^2\varphi$  in the BTZ background [13].

However it is known that one point functions of CFTs on a torus do acquire non-trivial expectation value. In [13], this expectation value was interpreted holographically as arising due to the cubic coupling of the field  $\varphi$  dual to the operator of interest with another bulk field  $\chi$ . More explicitly one considers the following action

$$S = \frac{1}{16\pi G_N} \int d^3x \sqrt{g} (\partial_\nu \varphi \partial^\nu \phi + m^2 \varphi^2 + \partial_\nu \chi \partial^\nu \chi + \mu^2 \chi^2 + g \chi^2 \varphi). \quad (5.1)$$

The field  $\chi^2$  acquires non-trivial expectation value due to the sum of propagators that wind around the horizon of the BTZ black hole, this in turn induces a one point function for the field  $\varphi$ . This is shown in figure 3.

In [3], the action in (5.1) was used to show that for the Schwarzschild BTZ black hole, the leading contribution to the expectation value of the operator  $\mathcal{O}$  dual to  $\varphi$  is given by

$$\lim_{\substack{m \rightarrow \infty - i\epsilon \\ L \rightarrow \infty}} \langle \mathcal{O} \rangle \sim (\text{powers of } m) \exp(-im\tau_s - m\ell_{\text{hor}}) \times e^{-\frac{2\pi L}{\beta}} + O\left(e^{-\frac{4\pi L}{\beta}}\right). \quad (5.2)$$

Here  $L$  is the periodicity in the spatial direction, when  $L \rightarrow \infty$ , the expectation value vanishes. In this section we will show that when one considers the BTZ black hole with rotation, the thermal one point function behaves as given in (5.2), where now  $\tau_s, \ell_{\text{hor}}$  are evaluated in the rotating BTZ geometry. Note that we do not see the occurrence of  $\ell_{\text{sing}}$ , the proper length from the inner horizon to the origin, unlike what was seen for the black hole with charge.

To see if this behaviour holds in other situations, we evaluate the expectation value of the composite made out of the bilinear  $\mathcal{O}^2$  in 2d CFT on a line but held at distinct left and right temperatures. The dual description of this CFT at large central charge is the BTZ black hole with angular momentum. Since the field is a composite, its expectation value at finite temperature is non-vanishing and can be obtained using conformal invariance. A closed expression can be obtained for this expectation value when the operator  $\mathcal{O}$  has large integer dimensions. We show that this expectation value can be written as

$$\lim_{m \rightarrow \infty - i\epsilon} \langle \mathcal{O}^2 \rangle \sim \exp(-2im\tau_s - 2m\ell_{\text{hor}}). \quad (5.3)$$

Again we do not see the appearance of the proper length  $\ell_{\text{sing}}$ . It will be interesting to see if this is a feature true for thermal one point functions in rotating black holes in higher dimensions.

### 5.1 Thermal one point function from gravity

We consider the BTZ metric with angular momentum which is given by

$$ds^2 = \frac{(-r^2 + r_-^2 + r_+^2) dt^2}{R^2} + \frac{r^2 R^2 dr^2}{(r^2 - r_-^2)(r^2 - r_+^2)} + r^2 d\phi^2 - \frac{2r_- r_+ dt d\phi}{R}. \quad (5.4)$$

Then by AdS/CFT, the expectation value of the operator dual to the scalar  $\varphi$  is given by

$$\langle \mathcal{O}(t, \phi) \rangle = g \int \sqrt{g} d^3 x' \langle \chi^2(x') \rangle K(x', t, \phi). \quad (5.5)$$

where  $K(x', t, \phi)$  is the bulk-boundary propagator of the  $\varphi$  field in the *BTZ* background, and the integral is carried out in the *BTZ* geometry outside the horizon. The expectation value  $\langle \chi^2(x') \rangle$  is obtained by considering the bulk-bulk propagator of the  $\chi$  field and subtracting the coincident limit singularity. We now provide the details for evaluation of the expectation value  $\chi^2$ , the bulk-boundary propagator  $K(x', t, \phi)$  and then proceed to evaluate the integral in (5.5).

**Bulk-Bulk propagator for  $\chi$ .** Bulk-Bulk propagators between 2 points in global *AdS*<sub>3</sub> are known exactly in terms of the geodesic distance between the points. Since the *BTZ* is a quotient of global *AdS*<sub>3</sub> through the identification  $\phi \rightarrow \phi + 2\pi$ , we first write down the geodesic length between the following two points at the same radial position and time coordinate in *BTZ* but at angular separation of  $\rho$ .

$$x_1 : (t, r, \phi = 0), \quad x_2 : (t, r, \phi = \rho). \quad (5.6)$$

The easiest approach to find the geodesic length is to use the embedding of the *BTZ* background into the hyperboloid defined by

$$-T_1^2 - T_2^2 + X_1^2 + X_2^2 = -R^2. \quad (5.7)$$

Then the *BTZ* black hole with angular momentum in (5.4) is obtained from the metric

$$ds^2 = -dT_1^2 - dT_2^2 + dX_1^2 + dX_2^2. \quad (5.8)$$

with the following embedding [26].

$$\begin{aligned} T_1 &= \sqrt{\frac{r^2 - r_+^2}{r_+^2 - r_-^2}} R \sinh\left(\frac{r_+ t - r_- R \phi}{R^2}\right), \\ T_2 &= \sqrt{\frac{r^2 - r_-^2}{r_+^2 - r_-^2}} R \cosh\left(\frac{r_+ R \phi - r_- t}{R^2}\right), \\ X_1 &= \sqrt{\frac{r^2 - r_+^2}{r_+^2 - r_-^2}} R \cosh\left(\frac{r_+ t - r_- R \phi}{R^2}\right), \\ X_2 &= \sqrt{\frac{r^2 - r_-^2}{r_+^2 - r_-^2}} R \sinh\left(\frac{r_+ R \phi - r_- t}{R^2}\right). \end{aligned} \quad (5.9)$$

From this relations, we see that the location of the 2 points in (5.6), in terms of the coordinates  $(T_1(x_i), T_2(x_i), X_1(x_i), X_2(x_i))$  can be obtained. Then the geodesic distance  $\hat{d}$  between these points is obtained using the relation

$$-R^2 \cosh \hat{d} = -T_1(x_1)T_2(x_2) - T_2(x_1)T_2(x_2) + X_1(x_1)X_1(x_2) + X_2(x_1)X_2(x_2). \quad (5.10)$$

We obtain the following simple formula for the geodesic distance between the points (5.6)

$$\cosh \hat{d} = \frac{(r_+^2 - r_-^2) \cosh(\frac{\rho r_+}{R}) + (r_+^2 - r_-^2) \cosh(\frac{\rho r_-}{R})}{r_+^2 - r_-^2}. \quad (5.11)$$

The bulk-bulk propagator in  $AdS_3$  is given by [27]

$$G_\Delta(u) = \frac{C_\Delta 2^\Delta}{u^\Delta} {}_2F_1\left(\Delta, \Delta - \frac{1}{2}, 2\Delta - 1, -\frac{2}{u}\right), \quad (5.12)$$

where

$$u = 2 \sinh^2 \frac{\hat{d}}{2} = \frac{(r_+^2 - r_-^2) \cosh(\frac{\rho r_-}{R}) + (r_+^2 - r_-^2) \cosh(\frac{\rho r_+}{R}) - (r_+^2 - r_-^2)}{r_+^2 - r_-^2}, \quad (5.13)$$

$$C_\Delta = \frac{\Gamma(\Delta)\Gamma(\Delta - \frac{1}{2})}{(4\pi)^{\frac{3}{2}}\Gamma(2\Delta - 1)}.$$

We will consider the case when the field  $\chi$  has conformal dimensions  $\Delta = 1$ , then

$$G_1(r, \rho) = \frac{1}{8\pi} \frac{1}{\sqrt{\frac{u}{2}(\frac{u}{2} + 1)}}. \quad (5.14)$$

Substituting for  $u$  from (5.13) we obtain

$$G_1(r, \rho) = \frac{1}{4\pi} \frac{(r_+^2 - r_-^2)}{\sqrt{[(r_+^2 - r_-^2) \cosh(\frac{r-\rho}{R}) + (r_+^2 - r_-^2) \cosh(\frac{r+\rho}{R})]^2 - (r_+^2 - r_-^2)^2}}. \quad (5.15)$$

Using this bulk to bulk propagator, we obtain

$$\langle \chi^2(r) \rangle = \sum_{n=-\infty, n \neq 0}^{\infty} G_1(2\pi n) = 2 \sum_{n=1}^{\infty} G_1(2\pi n). \quad (5.16)$$

Here we have removed the coincident singular limit and summed over all the windings to ensure periodicity in  $\phi \rightarrow \phi + 2\pi$ . Note that the expectation value of  $\chi^2$  just depends on the radial position.

**The bulk-boundary propagator for  $\varphi$ .** From the fact that the expectation value of  $\chi^2$  depends only the radial position, it is convenient to work in the Fourier expansion of the bulk-boundary propagator in frequency and the angle  $\phi$ . Let

$$K(r', t, t', \phi, \phi') = \sum_{n=-\infty}^{\infty} \int \frac{d\omega}{2\pi} e^{-i\omega(t-t') + in(\phi-\phi')} \hat{K}(r, r', \omega, n). \quad (5.17)$$

Then substituting this Fourier expansion in (5.5) and using the fact that  $\langle \chi^2(r) \rangle$  just depends on the radial position, we can perform the integral over  $t', \phi'$ . This leads to

$$\langle \mathcal{O}(x, t) \rangle = g \int_{r=r_+}^{\infty} r' dr' \hat{K}(r', 0, 0) \langle \chi^2(r') \rangle. \quad (5.18)$$

We obtain the zero mode of the bulk-boundary propagator  $\hat{K}(r', 0, 0)$  by examining the zero mode of the bulk-bulk Green's function, which satisfies the differential equation

$$\frac{1}{r} \partial_r \left( \frac{(r^2 - r_-^2)(r^2 - r_+^2)}{rR^2} \partial_r \hat{G}(r, r', 0, 0) \right) - m^2 \hat{G}(r, r', 0, 0) = \frac{\delta(r - r')}{r}. \quad (5.19)$$

We change variables to

$$x = \frac{r^2 - r_+^2}{r^2 - r_-^2}. \quad (5.20)$$

Then the differential equation for the Green's function reduces to

$$4(1-x)^2 \partial_x \left[ x \partial_x \hat{G}(x, x') \right] - m^2 R^2 \hat{G}(x, x') = \frac{2(1-x)^2 R^2}{r_+^2 - r_-^2} \delta(x - x'), \quad (5.21)$$

here it is understood that  $\hat{G}(x, x')$  refers to the Fourier zero mode along  $t, \phi$  directions.

We construct the Green's function by solving the homogenous equation. Let us define  $h = \frac{\Delta}{2}$ , which is related to the mass by

$$h = \frac{1}{2}(1 + \sqrt{1 + m^2 R^2}), \quad \nu = \sqrt{1 + m^2 R^2}. \quad (5.22)$$

The solution which is well behaved near the outer horizon  $r = r_+, x = 0$  is given by

$$\varphi_{\text{hor}} = (1-x)^{1-h} {}_2F_1(1-h, 1-h; 1; x), \quad (5.23)$$

and the solution which is well behaved at the boundary  $r = \infty, x = 1$  is given by

$$\varphi_{\text{inf}} = (1-x)^h {}_2F_1(h, h; 2h; 1-x). \quad (5.24)$$

Then the Green's function is given by

$$G(x, x') = A \times \left[ \varphi_{\text{inf}}(x) \varphi_{\text{hor}}(x') \theta(x - x') + \varphi_{\text{hor}}(x) \varphi_{\text{inf}}(x') \theta(x' - x) \right], \quad (5.25)$$

$$A = -\frac{R^2 \Gamma(h)^2}{2 \Gamma(2h) (r_+^2 - r_-^2)}.$$

We can now use the bulk-bulk Green's function to obtain the bulk-boundary Green's function. Substituting for  $z = \frac{R^2}{r}$  in (2.11) and then using (5.20) we obtain

$$K(x) = \lim_{x' \rightarrow 1} \frac{2\nu}{R^{4h}} \frac{(r_+^2 - r_-^2)^h}{(1-x')^h} G(x, x'), \quad (5.26)$$

$$= \frac{2\nu A}{R^{4h}} (r_+^2 - r_-^2)^h (1-x)^{1-h} {}_2F_1(1-h, 1-h; 1; x).$$

**Thermal one point function.** We are ready to substitute the necessary ingredients in (5.18) to obtain the one point function Using the bulk-boundary Green's function (5.26), the expectation value  $\langle \chi^2(r) \rangle$  from (5.15) we obtain

$$\langle \mathcal{O} \rangle = -\mathcal{K}(h) \sum_{n=1}^{\infty} \frac{1}{\sinh\left(\frac{2\pi nr_{\pm}}{R}\right)} \int_0^1 dx \frac{(1-x)^{h-1} {}_2F_1(h, h, 1; x)}{\sqrt{(1-\hat{\chi}_n^{(1)}x)(1-\hat{\chi}_n^{(2)}x)}}, \quad (5.27)$$

$$\mathcal{K}(h) = \frac{g\nu R^2}{4\pi} \frac{(r_+^2 - r_-^2)^h (\Gamma(h))^2}{R^{4h} \Gamma(2h)}.$$

where we have changed the integration variables to  $x$  using (5.20) and

$$\hat{\chi}_n^{(1)} = \frac{\cosh^2\left(\frac{\pi nr_-}{R}\right)}{\cosh^2\left(\frac{\pi nr_+}{R}\right)}, \quad \text{and} \quad \hat{\chi}_n^{(2)} = \frac{\sinh^2\left(\frac{\pi nr_-}{R}\right)}{\sinh^2\left(\frac{\pi nr_+}{R}\right)}. \quad (5.28)$$

In (5.27), we have used the fact that the expectation value of the operator is uniform from (5.18) and dropped the dependence on  $(t, \phi)$ . To take various limits it is convenient to change variables to  $w = 1 - x$  in (5.27) in the integrand, this results in

$$\langle \mathcal{O} \rangle = -\mathcal{K}(h) \sum_{n=1}^{\infty} \frac{1}{\sinh^2\left(\frac{\pi nr_+}{R}\right) - \sinh^2\left(\frac{\pi nr_-}{R}\right)} \int_0^1 dw \frac{w^{h-1} {}_2F_1(h, h, 1; 1-w)}{\sqrt{(1-\chi_n^{(1)}w)(1-\chi_n^{(2)}w)}}, \quad (5.29)$$

where

$$\chi_n^{(1)} = \frac{\hat{\chi}_n^{(1)}}{\hat{\chi}_n^{(1)} - 1} = \frac{\cosh^2\left(\frac{\pi nr_-}{R}\right)}{\sinh^2\left(\frac{\pi nr_-}{R}\right) - \sinh^2\left(\frac{\pi nr_+}{R}\right)}, \quad (5.30)$$

$$\chi_n^{(2)} = \frac{\hat{\chi}_n^{(2)}}{\hat{\chi}_n^{(2)} - 1} = \frac{\sinh^2\left(\frac{\pi nr_-}{R}\right)}{\sinh^2\left(\frac{\pi nr_-}{R}\right) - \sinh^2\left(\frac{\pi nr_+}{R}\right)}.$$

We can now expand the denominator in (5.29) using

$$\frac{1}{\sqrt{(1-\chi_1 w)(1-\chi_2 w)}} = \sum_{k=0}^{\infty} P_k \left( \frac{\chi_1 + \chi_2}{2\sqrt{\chi_1 \chi_2}} \right) (\sqrt{\chi_1 \chi_2} w)^k, \quad (5.31)$$

where  $P_k$  refers to the Legendre polynomial of order  $k$ . Substituting this expansion in (5.27), and integrating term by term we obtain

$$\langle \mathcal{O} \rangle = \mathcal{K}(h) \sum_{n=1, k=0}^{\infty} \frac{1}{\sinh^2\left(\frac{\pi nr_+}{R}\right) - \sinh^2\left(\frac{\pi nr_-}{R}\right)} \times \quad (5.32)$$

$$\left[ P_k \left( \frac{\chi_n^{(1)} + \chi_n^{(2)}}{2\sqrt{\chi_n^{(1)} \chi_n^{(2)}}} \right) \left( \sqrt{\chi_n^{(1)} \chi_n^{(2)}} \right)^k \frac{\Gamma(-h+k+1)\Gamma(h+k)}{\Gamma(k+1)^2} \right].$$

The above result is the closed form expression for the thermal one point function of the operator  $\mathcal{O}$ , in the rotating BTZ background which is induced by the cubic coupling with the field  $\chi$ . It will be interesting to compare this result with that of the CFT by developing the methods in [13]. This work assumed that the black hole could be modelled as a heavy state in the CFT, but the case when the heavy state had different left and right conformal dimensions was not considered.



$r_- \rightarrow 0$  limit. In [3], the one point function for the Schwarzschild BTZ was obtained. Let us first reproduce this results from the general expression (5.32). In the limit  $r_- \rightarrow 0$ , we see that

$$\begin{aligned} \chi_n^{(1)} &\rightarrow -\frac{1}{\sinh^2\left(\frac{\pi nr_+}{R}\right)} \quad \text{and} \quad \chi_n^{(2)} \rightarrow 0, \\ P_k\left(\frac{\chi_n^{(1)} + \chi_n^{(2)}}{2\sqrt{\chi_n^{(1)}\chi_n^{(2)}}}\right) \left[\sqrt{\chi_n^{(1)}\chi_n^{(2)}}\right]^k &\rightarrow \frac{\Gamma(2k+1)}{4^k\Gamma(k+1)^2} (\chi_n^{(1)})^k, \\ \mathcal{K}(h) &\rightarrow \frac{g\nu R^2}{4\pi} \frac{r_+^{2h}\Gamma(h)^2}{R^{4h}\Gamma(2h)}. \end{aligned} \tag{5.33}$$

Substituting these leading terms in (5.32), we obtain

$$\begin{aligned} \langle \mathcal{O} \rangle &= \frac{g\nu R^2}{4\pi} \frac{\Gamma(h)^2}{z_0^{2h}\Gamma(2h)} \times \\ &\sum_{n=1, k=0}^{\infty} \frac{1}{\sinh^2\left(\frac{\pi nr_+}{R}\right)} \frac{\Gamma(2k+1)}{4^k\Gamma(k+1)^2} (\chi_n^{(1)})^k \frac{\Gamma(-h+k+1)\Gamma(h+k)}{\Gamma(k+1)^2}, \\ &= \frac{g\nu R^2}{4\pi} \frac{\Gamma(h)^2}{z_0^{2h}\Gamma(2h)} \sum_{n=1}^{\infty} \frac{\pi \csc(\pi h)}{\sinh^2\left(\frac{\pi nr_+}{R}\right)} {}_3F_2\left(\frac{1}{2}, 1-h, h; 1, 1; -\frac{1}{\sinh^2\left(\frac{\pi nr_+}{R}\right)}\right). \end{aligned} \tag{5.34}$$

To obtain the second line, we have used the Legendre duplication formula to simplify the Gamma functions in the numerator and then used the definition of the hypergeometric function  ${}_3F_2$  to sum over  $k$ . We have also replaced  $\frac{R^2}{r_+}$  by  $z_0$ . The last line in (5.34), is the expression obtained in [3] for thermal one point function in the Schwarzschild BTZ background.

To interpret the one point function geometrically, we first take the limit  $\frac{2\pi r_+}{R} \rightarrow \infty$ . At this point it is instructive to relate this limit to the one taken in [3], in which the length of the identification in the spatial direction of the BTZ black hole is large. To do this let us write the metric of the BTZ Schwarzschild metric from (5.4)

$$ds^2 = \frac{R^2}{z^2} \left[ \left(1 - \frac{z^2}{z_0^2}\right) dt^2 + \frac{dz^2}{1 - \frac{z^2}{z_0^2}} + R^2 d\varphi^2 \right]. \tag{5.35}$$

Here we have written the Euclidean BTZ, in which  $t$  is identified as  $t \rightarrow t + \beta$ , where

$$z_0 = \frac{R^2}{r_+} = \frac{\beta}{2\pi}, \tag{5.36}$$

On re-defining the co-ordinates as

$$z' = \frac{z}{z_0}, \quad t' = \frac{t}{z_0}, \quad x = \frac{R}{z_0} \phi. \tag{5.37}$$

the metric becomes

$$ds^2 = \frac{R^2}{z'^2} \left[ (1 - z'^2) dt'^2 + \frac{dz'^2}{1 - z'^2} + dx^2 \right]. \tag{5.38}$$

With this scaling, we have the identifications

$$t' \sim t' + 2\pi, \quad x \sim x + 2\pi \frac{2\pi R}{\beta}. \quad (5.39)$$

To arrive at the identification in  $x$  we have used the relation between  $z_0$  and  $\beta$  in (5.36). This is the rescaled co-ordinates used in [3]. The periodicity in the spatial direction can be read from (5.35). It is given by to be  $L = 2\pi R$  and therefore  $x \sim x + \frac{2\pi L}{\beta}$ . Let us now examine the ratio  $\frac{r_{\pm}}{R}$ , from (5.36)

$$\frac{2\pi r_+}{R} = 2\pi \frac{2\pi R}{\beta} = \frac{2\pi L}{\beta}, \quad (5.40)$$

Therefore taking the limit

$$\frac{2\pi r_+}{R} \rightarrow \infty \quad (5.41)$$

corresponds to the same limit of large spatial periodicities of [3].

Examining the one point function in (5.34) in the limit (5.41), we see only the  $n = 1$  term contributes and we can also just retain the leading term from the hypergeometric function which results in

$$\langle \mathcal{O} \rangle = \frac{g\nu R^2}{2} \frac{\Gamma(h)^2}{z_0^{2h} \Gamma(2h)} \csc(\pi h) e^{-\frac{2\pi r_+}{R}}. \quad (5.42)$$

Note that the  $z_0^{-2h}$  just provides the scaling dimensions for the expectation value. In this form it is easy to see that on further taking the limit  $h \rightarrow \infty - i\epsilon$

$$\begin{aligned} \lim_{h \rightarrow \infty - i\epsilon} \langle \mathcal{O} \rangle &\sim e^{-i\pi h} 2^{-2h} e^{-\frac{2\pi r_+}{R}}, \\ &\sim e^{-i\pi \frac{mR}{2}} 4^{-\frac{mR}{2}} e^{-\frac{2\pi r_+}{R}}. \end{aligned} \quad (5.43)$$

To obtain the last line we have used (5.22) to replace  $h$  in terms of the mass  $m$ . Comparing the coefficient of  $e^{-\frac{2\pi r_+}{R}}$  in (2.26), we see that it behaves just as seen for thermal one point functions in higher dimensions.

**Limit  $\frac{r_-}{R}, \frac{r_+}{R} \rightarrow \infty$ , with  $\frac{r_-}{r_+}$  held fixed.** In this limit, we still can keep track of the dependence of the one point function on the inner horizon. Before we take this limit, it is convenient to simplify the dependence on  $r_-, r_+$  in (5.32). We can write

$$\frac{\chi_n^{(1)} + \chi_n^{(2)}}{2\sqrt{\chi_n^{(1)} \chi_n^{(2)}}} = \coth \frac{2\pi n r_-}{R}, \quad (5.44)$$

and

$$\sqrt{\chi_n^{(1)} \chi_n^{(2)}} = \frac{\sinh \frac{2\pi n r_-}{R}}{\cosh \frac{2\pi n r_-}{R} - \cosh \frac{2\pi n r_+}{R}}. \quad (5.45)$$

We need the limit

$$\lim_{\frac{r_-}{R} \rightarrow \infty} P_k \left( \coth \frac{2\pi n r_-}{R} \right) = 1 + O\left(\exp\left(-\frac{4\pi n r_-}{R}\right)\right). \quad (5.46)$$

We substitute (5.44), (5.45) into the expression for the one point function in (5.32) and take the limit

$$\frac{r_-}{R} \rightarrow \infty, \quad \frac{r_+}{R} \rightarrow \infty, \quad \frac{r_-}{r_+} = \delta \text{ fixed.} \quad (5.47)$$

Using (5.46), we see that the leading contribution arises from  $n = 1, k = 0$  term in the sum. All the remaining terms are exponentially suppressed compared to this term, which is given by

$$\begin{aligned} \langle \mathcal{O} \rangle &= \frac{g\nu R^2}{2} \frac{(r_+^2 - r_-^2)^h \Gamma(h)^2}{R^{4h} \Gamma(2h)} \csc(\pi h) e^{-\frac{2\pi r_+}{R}} + O\left[\exp\left(-\frac{2\pi r_+}{R}(2 - \delta)\right)\right], \\ &= \frac{g\nu R^2}{2} \frac{\Gamma(h)^2}{z_0^{2h} \Gamma(2h)} \csc(\pi h) e^{h \log(1 - \delta^2)} e^{-\frac{2\pi r_+}{R}}, \end{aligned} \quad (5.48)$$

with  $z_0 = \frac{R^2}{\sqrt{r_+^2 - r_-^2}}$ .

Finally we can take the  $h \rightarrow \infty - i\epsilon$

$$\begin{aligned} \lim_{h \rightarrow \infty - i\epsilon} \langle \mathcal{O} \rangle &\sim e^{-i\pi h} e^{-h(\log 4 - \log(1 - \delta^2))} e^{-\frac{2\pi r_+}{R}}, \\ &= e^{-i\frac{\pi m R}{2}} e^{-\frac{m R}{2}(\log 4 - \log(1 - \delta^2))} e^{-\frac{2\pi r_+}{R}}. \end{aligned} \quad (5.49)$$

**Comparison with geometric lengths.** From the metric (5.4, the time to singularity is given by the integral

$$\begin{aligned} \tau_s &= R \int_{r_-}^{r_+} \frac{r dr}{\sqrt{(r_+^2 - r^2)(r^2 - r_-^2)}}, \\ &= \frac{R\pi}{2}. \end{aligned} \quad (5.50)$$

The proper length from infinity to the horizon is given by

$$\begin{aligned} \hat{\ell}_{\text{hor}} &= \lim_{\epsilon \rightarrow 0} R \int_{r_+}^{\frac{R^2}{\epsilon}} \frac{r dr}{\sqrt{(r_+^2 - r^2)(r^2 - r_-^2)}}, \\ &= -\frac{R}{2} \log(1 - \delta^2) + R \log(2) - \log \frac{\epsilon}{z_0}, \quad z_0 = \frac{R^2}{r_+}. \end{aligned} \quad (5.51)$$

Here we have chosen the same cut off as in (2.28), since  $r$  and  $z$  are related by  $r = \frac{R^2}{z}$ . Therefore the regularized proper length is given by

$$\hat{\ell}_{\text{hor}} = -\frac{R}{2} \log(1 - \delta^2) + R \log(2). \quad (5.52)$$

Finally one can also evaluate the proper length from the inner horizon to the singularity, we obtain

$$\hat{\ell}_{\text{sing}} = \frac{R}{2} \log\left(\frac{1 - \delta}{1 + \delta}\right). \quad (5.53)$$

Comparing the leading contribution to the thermal one point function in (5.49) with these geometric lengths, we see that it can be written as

$$\langle \mathcal{O} \rangle \sim \exp(-im\tau_s - m\ell_{\text{hor}}) e^{-\frac{2\pi r_+}{R}}. \quad (5.54)$$

Note that in the limit (5.47) we do not see the presence of  $\ell_{\text{hor}}$ , the proper length from the inner horizon to the singularity.

## 5.2 One point function $\langle \mathcal{O}^2 \rangle$ from CFT

From the analysis of the rotating BTZ background we saw that in the large horizon radius limit, or the large spatial length limit, the leading contribution to the thermal one point function does not see  $\ell_{\text{sing}}$ , the geometric length from the inner horizon to the singularity. We know that composite operators, or operators which do not transform as conformal primaries gain thermal expectation value in 2d CFT on a plane. In this section we evaluate this one point function and observe that when their conformal dimensions are large, their expectation value can be cast into the geometric form, but again there is no information about  $\ell_{\text{sing}}$ .

We consider the bilinear composite  $\mathcal{O}^2$  of the primary  $\mathcal{O}$  of dimension  $2h_{\mathcal{O}}$  and let  $2h_{\mathcal{O}}$  be an integer. Here the holomorphic and the anti-holomorphic dimension of the operator is  $(h_{\mathcal{O}}, h_{\mathcal{O}})$ . The one point function of the operator of the composite can be obtained by the following approach. We first look at the 2 point function at finite temperature

$$\langle \mathcal{O}(w, \bar{w}) \mathcal{O}(0, 0) \rangle = \left[ \frac{\beta_L}{\pi} \sinh \left( \frac{\pi w}{\beta_L} \right) \right]^{-2h_{\mathcal{O}}} \left[ \frac{\beta_R}{\pi} \sinh \left( \frac{\pi \bar{w}}{\beta_R} \right) \right]^{-2h_{\mathcal{O}}}. \quad (5.55)$$

Here the left and right inverse temperatures of the CFT is given by  $(\beta_L, \beta_R)$  and since we are interested in the BTZ black hole with angular momentum we should have  $\beta_L \neq \beta_R$ . The expectation value  $\langle \mathcal{O}^2 \rangle$  can be obtained by examining the expansion in  $w, \bar{w}$  of (5.55) and extracting out the constant term. To see that this indeed captures thermal expectation value, we know that the OPE of  $\mathcal{O}$  with itself contains the composite  $\mathcal{O}^2$ .

$$\mathcal{O}(z, \bar{z}) \mathcal{O}(0, 0) \sim \frac{1}{|z|^{4h_{\mathcal{O}}}} + \dots + C \mathcal{O}^2(0, 0) + \dots. \quad (5.56)$$

Here the  $\dots$  refer to other singular terms or terms which depend on powers of  $z, \bar{z}$  in the OPE which we are not interested in. The  $\mathcal{O}^2$  operator occurs in the OPE with no dependence of  $z$  and  $C$  is the OPE coefficient. Now taking thermal expectation value on both sides of this equation, we see that the constant term, independent of  $z, \bar{z}$  is proportional to the expectation value  $\langle \mathcal{O}^2 \rangle$ . To extract the constant term, it is sufficient to look at the holomorphic two point function and obtain the residue in the Laurent expansion in  $z$ . The residue when  $2h_{\mathcal{O}}$  is an integer is given by

$$a_0(\beta) = \frac{1}{2\pi i} \oint \frac{dw}{w} \left[ \frac{\beta}{\pi} \sinh \left( \frac{\pi w}{\beta} \right) \right]^{-2h_{\mathcal{O}}}, \quad (5.57)$$

where the integral is around the origin. Then from the OPE expansion of (5.55), the thermal expectation value is given by

$$C \langle \mathcal{O}^2 \rangle = a_0(\beta_L) a_0(\beta_R). \quad (5.58)$$

Examining the residue (5.57), we see that it is non-zero only when  $2h_{\mathcal{O}}$  is an even integer or  $h_{\mathcal{O}}$  is an integer. We re-write the residue as

$$a_0(\beta) = \frac{1}{2\pi i} \left( \frac{\pi}{\beta} \right)^{2h_{\mathcal{O}}} \oint dy e^{-[\log y + 2h_{\mathcal{O}} \log(\sinh y)]}. \quad (5.59)$$

$h_{\mathcal{O}}$	$(a_0 \beta^{2h_{\mathcal{O}}} \pi^{\frac{1}{2}-2h_{\mathcal{O}}})$ Exact	$(a_0 \beta^{2h_{\mathcal{O}}} \pi^{\frac{1}{2}-2h_{\mathcal{O}}})$ Saddle point	Error in %
5	-0.280338	-0.279105	0.439624
10	0.199763	0.199308	0.227946
15	-0.163527	-0.163275	0.153875
20	0.141801	0.141637	0.116138
25	-0.126929	-0.126811	0.0932657
30	0.11593	0.11584	0.07792
35	-0.10737	-0.107298	0.0669107
40	0.100463	0.100404	0.0586273
45	-0.0947381	-0.0946887	0.052169
50	0.089892	0.0898497	0.0469923
55	-0.0857207	-0.0856841	0.0427502
60	0.082081	0.0820488	0.0392106
65	-0.0788687	-0.0788402	0.0362124

**Table 1.** Numerical comparison of the exact value of the residue at integer  $h_{\mathcal{O}}$  against the saddle point given in (5.61).

For large  $2h_{\mathcal{O}}$  we can perform this integral by the saddle point method. The saddle points at the leading order are at

$$y_{\text{saddle}} = \pm \frac{i\pi}{2} + O\left(\frac{1}{h_{\mathcal{O}}}\right). \tag{5.60}$$

Adding the contributions at the 2 saddles along with the one loop term at each of the saddles we obtain

$$a_0(\beta) = \frac{1}{2\pi i} \oint \frac{dw}{w} \left( \frac{\beta}{\pi} \sinh \left[ \frac{\pi w}{\beta} \right] \right)^{-2h_{\mathcal{O}}} \approx \frac{2\pi^{2h_{\mathcal{O}}-\frac{1}{2}} \cos(\pi h_{\mathcal{O}})}{\beta^{2h_{\mathcal{O}}} \sqrt{2 + \pi^2 h_{\mathcal{O}}}}. \tag{5.61}$$

We can compare the value of  $a_0$  from the saddle point against the numerical value, which can be obtained by explicitly evaluating the residue. This comparison is shown in the table 1 as well as in the graph in figure 4, we see that indeed, that the saddle point approximation is a good approximation at large values of integer  $2h_{\mathcal{O}}$ .

From the approximation of  $a_0(\beta)$  in (5.61), we see that the thermal one point function is given by in the large  $2h_{\mathcal{O}}$  limit is given by

$$\begin{aligned} \langle \mathcal{O}^2 \rangle &= \frac{1}{C} a_0(\beta_L) a_0(\beta_R), \\ &= \frac{1}{C} \left( \frac{1}{\beta_L \beta_R} \right)^{2h_{\mathcal{O}}} \frac{4\pi^{4h_{\mathcal{O}}-1} \cos^2(\pi h_{\mathcal{O}})}{2 + \pi^2 h_{\mathcal{O}}}. \end{aligned} \tag{5.62}$$

The  $\cos^2(\pi h_{\mathcal{O}})$  term is just unity when  $h_{\mathcal{O}}$  is an integer, but we keep this factor so that it enables us to obtain the general form of the result. Let us now recast this expression in terms of geometric quantities in the bulk. The left and right inverse temperatures are related to the horizon radii by [28]

$$\frac{1}{\beta_L} = \frac{r_+ - r_-}{2\pi R^2}, \quad \frac{1}{\beta_R} = \frac{r_+ + r_-}{2\pi R^2}. \tag{5.63}$$

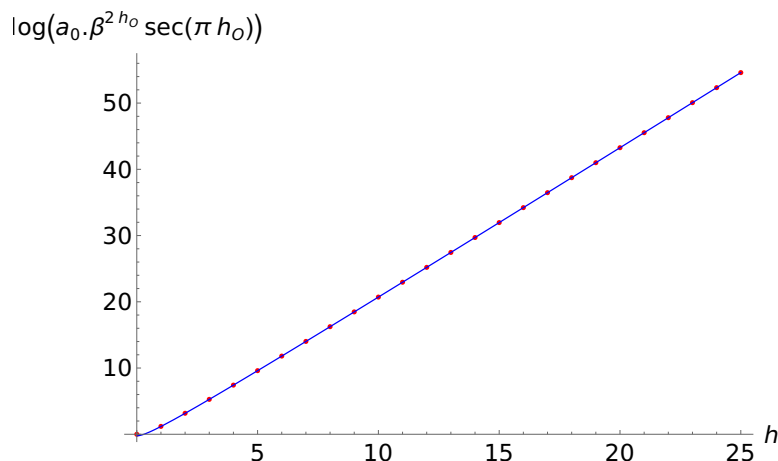


**Figure 4.** The blue curve represents the plot of the function  $\log[a_0 \beta^{2h_\mathcal{O}} \sec(\pi h_\mathcal{O})]$ , where  $a_0$  is obtained from the result of our saddle point analysis given in the equation (5.61). The red points are the exact values of the  $\log[a_0 \beta^{2h_\mathcal{O}} (-1)^{h_\mathcal{O}}]$  at the integer values of  $h_\mathcal{O}$  obtained by explicitly evaluating the residue (5.57).

Using this relation in (5.62), we can write

$$\lim_{h_\mathcal{O} \rightarrow \infty + i\epsilon} \langle \mathcal{O}^2 \rangle \sim \frac{1}{C z_0^{4h_\mathcal{O}}} e^{-2h_\mathcal{O} \log 4 + 2h_\mathcal{O} \log(1-\delta^2)} \exp(-i2\pi h_\mathcal{O}). \quad (5.64)$$

The small imaginary part selects the leading phase to be  $\exp(-2\pi i h_\mathcal{O})$ . In gravity the 3 OPE coefficient is given by  $C = \sqrt{2}$  [29], therefore they does not grow exponentially in  $h_\mathcal{O}$ . We can also identify  $2h_\mathcal{O} = \frac{\Delta_{\mathcal{O}^2}}{2}$ . With these inputs, the thermal one point function can be written as

$$\begin{aligned} \langle \mathcal{O}^2 \rangle &\sim \exp \left[ -i\pi \frac{\Delta_{\mathcal{O}^2}}{2} - \frac{\Delta_{\mathcal{O}^2}}{2} (\log 4 - \log(1 - \delta^2)) \right], \\ &\sim \exp \left[ -i \frac{\pi 2mR}{2} - \frac{2mR}{2} (\log 4 - \log(1 - \delta^2)) \right]. \end{aligned} \quad (5.65)$$

Using (5.50), (5.52), we can write the expectation value of the composite as

$$\langle \mathcal{O}^2 \rangle \sim e^{-i2m\tau_s - 2m\ell_{\text{hor}}}. \quad (5.66)$$

Note that  $m \rightarrow 2m$  since we are evaluating the expectation value of the composite  $\mathcal{O}^2$ , and we do not see the appearance of  $\ell_{\text{sing}}$ .

Though our calculation in the CFT has been done only for integer conformal dimensions, we have written the result so that it is natural to read out the general form of the result. But, it will be interesting to see if the methods of [30] can be used to verify if indeed the expectation value of the composite can be written in the form for arbitrary conformal dimensions.<sup>6</sup>

---

<sup>6</sup>In [30] the expectation value of the composite in which the operator  $\mathcal{O}$  obeys mean field theory correlators have been written for 2d CFT, but not for the correlator given in (5.55). We have verified that the expectation value of the composite  $\mathcal{O}^2$  using the mean field theory correlator does not behave as in (5.62) in the large  $h_\mathcal{O}$  limit.

## 6 Conclusions

We have discussed two examples in which the thermal one point function of massive scalars can be evaluated exactly. For the charged planar black hole we introduced a large  $d$  limit to achieve this. In both these examples the result for the one point function agreed with that anticipated in [3] using WKB methods. In particular for the charged black hole which has an inner horizon we observed the presence of  $\ell_{hor}$ , the proper distance from the inner horizon to the singularity. The second example involved hyperbolic black holes for which  $\tau_s$ , the time to the singularity has a different dependence on the radius of  $AdS_{d+1}$ . We also saw that these results remain the same for both the Gauss-Bonnet or the Weyl tensor squared coupling.

We obtained the one point function of massive scalars in BTZ due to a cubic coupling of scalars. We could interpret this result geometrically in a suitable limit of large horizon radius, but could not find the dependence of  $\ell_{sing}$  in this limit. It would be interesting to investigate the case of rotating black hole in higher dimensions. The WKB methods of [3] assumed radial symmetry and it would be important to generalize those arguments to backgrounds with axial symmetry. The recent developments [31, 32] regarding the applications of the solutions to the Heun equation to evaluate thermal 2 point functions will be helpful in this regard.

We saw that in  $2d$  we could gain some insight on thermal one point functions by evaluating the expectation value of composite scalars at finite temperature. For this we used integer conformal dimensions. The methods of [30] can be used to study this question for arbitrary conformal dimensions. It will be important to develop such methods in field theory to understand the features of thermal one point function. As we have seen, these contain some information of the geometry behind the horizon and evaluating one thermal one point functions directly in the dual field theory can give us new insight to black hole geometry.

## Acknowledgments

We thank Chethan Krishnan, Suvrat Raju and Aninda Sinha for discussions during the presentation of a preliminary version of this work. J.R.D thanks the group at the Asia Pacific Center for Theoretical Physics, Pohang for the warm hospitality during the completion of this work.

## A Details for the Green's function

The bulk-bulk Green's function  $G(z, z')$  satisfies the equation,

$$\partial_z \left( \frac{R^{d-1}}{z^{d-1}} f(z) \partial_z G(z, z') \right) - \frac{R^{d-1}}{z^{d-1}} m^2 G(z, z') = \delta(z - z'), \quad (\text{A.1})$$

and  $G(z, z')$  has to be well-behaved at the boundaries  $z = 0$  and  $z = z_0$ ;  $f(z)$  was defined in the equation (2.7).

Now, the two linearly independent solutions of the homogeneous part of the differential equation (A.1) are given by,

$$g_{\text{inf}}(w) = w^h {}_2F_1(h, h, 2h, w), \quad \text{and}, \quad g_{\text{hor}}(w) = w^h {}_2F_1(h, h, 1, 1-w). \quad (\text{A.2})$$

$$\text{Where,} \quad w = \left(\frac{z}{z_0}\right)^d, \quad h = \frac{\Delta}{d}, \quad (\text{A.3})$$

The solutions  $g_{\text{inf}}(w)$  and  $g_{\text{hor}}(w)$  are regular at  $w = 0$  and at  $w = 1$  respectively, which indicates,

$$G(w, w') = \begin{cases} A(w')g_{\text{inf}}(w) & \text{for } w < w', \\ B(w')g_{\text{hor}}(w) & \text{for } w > w'. \end{cases} \quad (\text{A.4})$$

Where  $A(w')$  and  $B(w')$  are functions of  $w'$ , to be determined.

Now, for the Green's function to be continuous at  $w = w'$ , we should have,

$$A(w')g_{\text{inf}}(w') = B(w')g_{\text{hor}}(w'). \quad (\text{A.5})$$

The jump of  $\partial_w G(w, w')$  around  $w = w'$  is obtained by integrating the both side of the equation (A.1) with respect to  $z$  from  $z = z' - \epsilon$  to  $z = z' + \epsilon$  with  $\epsilon \rightarrow 0$  and then we used the equation (A.5) to get,

$$\frac{B(w')}{g_{\text{inf}}(w')} \left( g_{\text{inf}}(w')g'_{\text{hor}}(w') - g_{\text{hor}}(w')g'_{\text{inf}}(w') \right) = \frac{z_0^d}{R^{d-1}d(1-w)}. \quad (\text{A.6})$$

Note that the terms inside the parenthesis in the l.h.s. is equal to the Wronskian of the homogeneous part of the differential equation (A.1) written in  $w'$  variable. And this Wronskian is calculated up to an overall constant factor  $\tilde{C}$  directly from the differential equation, thus we have,

$$\left( g_{\text{inf}}(w')g'_{\text{hor}}(w') - g_{\text{hor}}(w')g'_{\text{inf}}(w') \right) = \frac{\tilde{C}}{1-w'}. \quad (\text{A.7})$$

Now, the constant  $\tilde{C}$  is determined by expanding the both side of the above equation in the taylor series about  $w = 0$ . The first term of the series expansion of the l.h.s. is equal to  $\tilde{C}$ . Thus one obtains,

$$\tilde{C} = -\frac{\Gamma(2h)}{\Gamma(h)^2}. \quad (\text{A.8})$$

Hence,

$$B(w') = -\frac{\Gamma(h)^2}{\Gamma(2h)} \frac{z_0^d}{R^{d-1}d} g_{\text{inf}}(w'), \quad A(w') = -\frac{\Gamma(h)^2}{\Gamma(2h)} \frac{z_0^d}{R^{d-1}d} g_{\text{hor}}(w'). \quad (\text{A.9})$$

And finally, the bulk-bulk green's function,

$$G(w, w') = -\frac{\Gamma(h)^2}{\Gamma(2h)} \frac{z_0^d}{R^{d-1}d} \left( g_{\text{inf}}(w)g_{\text{hor}}(w')\theta(w' - w) + g_{\text{hor}}(w)g_{\text{inf}}(w')\theta(w - w') \right).$$



## B The charged planar black hole solution at large $d$

The consistency of the treatment of large  $d$  limit used to evaluate the one point function for the case of the charged planar black hole requires the metric (3.1) in this limit to satisfy the Einstein-Maxwell field equation at the leading order in  $d$ . In this appendix, we will verify it by straightforward calculation.

At the limit described in (3.5), the metric (3.1) takes the form,

$$ds^2 \approx \frac{R_{\text{AdS}}^2}{z^2} \left( -\hat{f}(z)dt^2 + \frac{dz^2}{\hat{f}(z)} + d\vec{x}^2 \right), \quad \text{where} \quad \hat{f}(z) = 1 - \frac{z^d}{z_0^d} + Q \frac{z^{2d}}{z_0^{2d}}. \quad (\text{B.1})$$

Note that the asymptotic behaviour of the metric at the boundary is kept intact in this limit, thus the rules of AdS/CFT were implemented to obtain the one-point function.

The above metric should satisfy the following Einstein-Maxwell field equation at large  $d$ ,

$$\lim_{d \rightarrow \infty} \left( R_{\mu\nu} - \frac{1}{2}g_{\mu\nu}R - \Lambda g_{\mu\nu} \right) = - \lim_{d \rightarrow \infty} 8\pi T_{\mu\nu}, \quad (\text{B.2})$$

where the cosmological constant  $\Lambda = -\frac{d(d-1)}{2R_{\text{AdS}}^2}$  for the  $AdS_{d+1}$  and  $T_{\mu\nu}$  is the energy-momentum stress tensor evaluated from the gauge potential [18],

$$A = \left( -\frac{qz^{d-2}}{c} + \Phi \right) dt, \quad \Phi \text{ is constant, and} \quad c = \sqrt{\frac{2(d-2)}{d-1}}. \quad (\text{B.3})$$

By calculating the l.h.s. and r.h.s. separately for each tensorial component of the equation (B.2), after incorporating the metric (B.1) in it, we will show that l.h.s.=r.h.s. for each component. For this calculation we need the following results,

$$R_{00} = \frac{f(z)(-2f(z)d + z[(1+d)f'(z) - zf''(z)])}{2z^2}, \quad (\text{B.4})$$

$$R_{11} = \frac{2f(z)d + z[-(d+1)f'(z) + zf''(z)]}{2z^2 f(z)}, \quad (\text{B.5})$$

$$R_{ii} = \frac{df(z) - zf'(z)}{z^2} \quad \text{for } i \in [2, d]. \quad (\text{B.6})$$

All other components of Ricci-tensor are zero. And the Ricci-scalar is given by,

$$R = d(d+1)f(z) + z(-2f'(z)d + zf''(z)). \quad (\text{B.7})$$

For the 00-component,

$$\begin{aligned} \lim_{d \rightarrow \infty} \left( R_{00} - \frac{1}{2}g_{00}R - \Lambda g_{00} \right) &= \lim_{d \rightarrow \infty} \left( -\frac{d(d-1)}{2} Q z^{2d-2} z_0^{-4d} [Q z^{2d} + z_0^d (-z^d + z_0^d)] \right), \\ &= \frac{1}{z^2} \left[ -e^{2d \log(\frac{z}{z_0})} + e^{3d \log(\frac{z}{z_0})} - e^{4d \log(\frac{z}{z_0})} \right]. \end{aligned} \quad (\text{B.8})$$

$$\begin{aligned} - \lim_{d \rightarrow \infty} 8\pi T_{00} &= - \lim_{d \rightarrow \infty} \left( \frac{(d-2)(d-1)}{2} Q z^{2d-4} z_0^{2-4d} [Q z^{2d} + z_0^d (-z^d + z_0^d)] \right), \\ &= \frac{1}{z^2} \left[ -e^{2d \log(\frac{z}{z_0})} + e^{3d \log(\frac{z}{z_0})} - e^{4d \log(\frac{z}{z_0})} \right]. \end{aligned} \quad (\text{B.9})$$

For the 11-component,

$$\begin{aligned} \lim_{d \rightarrow \infty} \left( R_{11} - \frac{1}{2} g_{11} R - \Lambda g_{11} \right) &= \lim_{d \rightarrow \infty} \frac{d(d-1)Qz^{2d-2}}{2(Qz^{2d} + z_0^2 d - z^d z_0^d)}, \\ &= \frac{1}{z^2} \left( \frac{1}{e^{2d \log(\frac{z_0}{z})} - e^{d \log(\frac{z_0}{z})} + Q} \right). \end{aligned} \quad (\text{B.10})$$

$$\begin{aligned} - \lim_{d \rightarrow \infty} 8\pi T_{11} &= \lim_{d \rightarrow \infty} \left( \frac{(d-2)(d-1)Qz_0^2}{2z^4[Q + z^{-2d}z_0^d(-z^d + z_0^d)]} \right), \\ &= \frac{1}{z^2} \left( \frac{1}{e^{2d \log(\frac{z_0}{z})} - e^{d \log(\frac{z_0}{z})} + Q} \right). \end{aligned} \quad (\text{B.11})$$

and, for  $ii$ -component,

$$\begin{aligned} \lim_{d \rightarrow \infty} \left( R_{ii} - \frac{1}{2} g_{ii} R - \Lambda g_{ii} \right) &= - \lim_{d \rightarrow \infty} \left( \frac{d(d+1)Qz^{2d-2}z_0^{-2d}}{2} \right), \\ &= - \frac{1}{z^2} e^{2d \log(\frac{z}{z_0})}. \end{aligned} \quad (\text{B.12})$$

$$\begin{aligned} - \lim_{d \rightarrow \infty} 8\pi T_{ii} &= \lim_{d \rightarrow \infty} \left( - \frac{(d-2)(d-1)Qz^{2d-4}z_0^{2-2d}}{2} \right), \\ &= - \frac{1}{z^2} e^{2d \log(\frac{z}{z_0})}. \end{aligned} \quad (\text{B.13})$$

Thus, for each tensorial component we have shown that l.h.s. = r.h.s., i.e., the Einstein-Maxwell field equation is satisfied by the metric given in (B.1) at the leading order in  $d$ .

### C Large $d$ with Weyl tensor squared coupling

We repeat the calculation for the one point function in the charged planar black hole background at large  $d$ , described in section 3, but using the Weyl tensor squared coupling in place of the GB coupling.

The rules of AdS/CFT prescribe the one point function to be,

$$\langle O(t, \vec{x}) \rangle = \alpha \int dz dt' d\vec{x}' \sqrt{g} \tilde{K}(t, \vec{x}; z, t', \vec{x}') W^2(z, t', \vec{x}'), \quad (\text{C.1})$$

where the  $W^2 = W_{\mu\nu\rho\sigma} W^{\mu\nu\rho\sigma}$ , and it would be sufficient to do only the  $z$  part of the above integral as was argued before.

For the metric given in (3.1),

$$W^2 = \frac{(d-2)(d-1)^2 w^{2-\frac{4}{d}} [(6-4d)Qw + dw^{2/d}]^2}{R^4 d}. \quad (\text{C.2})$$

And in the limit  $d \rightarrow \infty$ , the leading contribution to the Weyl tensor's square is given by,

$$W^2 = \frac{w^2(1-4Qw)^2 d^4}{R^4}. \quad (\text{C.3})$$

Now plugging the expression for the bulk-boundary green's function  $K(w)$ , given in (3.12), in the equation (C.1), and using the change of variable defined in (3.16), we get,

$$\begin{aligned} \langle O \rangle = & -\frac{4d^2(1-4Q)^{h/2}}{R^2} \frac{(\Gamma(h))^2}{\Gamma(2h)} \left(\frac{2\nu}{z_0^{\Delta_+}}\right) \int_0^1 dy (1-y)^h {}_2F_1(h, h, 1, y) \times \\ & \left[ (2Qw_+)^{-2} (1-\chi y)^{-2} - 16Q(2Qw_+)^{-3} (1-y)(1-\chi y)^{-3} \right. \\ & \left. + 64Q^2(2Qw_+)^{-4} (1-y)^2 (1-\chi y)^{-4} \right]. \end{aligned} \tag{C.4}$$

Applying the integration formulae used in the section 3, the integrals in the above equation are performed to get the analytic expression for the thermal one point function,

$$\begin{aligned} \langle O \rangle = & -\frac{4d^2(1-4Q)^{\frac{h}{2}-1}}{R^2} \frac{(\Gamma(h))^2}{\Gamma(2h)} \frac{h(h-1)\pi \csc(\pi h)}{12(1-\sqrt{1-4Q})} \left(\frac{2\nu}{z_0^{\Delta_+}}\right) \times \\ & \left( \left[ 3(-1+\sqrt{1-4Q}) + 8Q(h-2)\{h(-1+\sqrt{1-4Q}) + \sqrt{1-4Q}\} \right] \right. \\ & \times {}_2F_1\left(2-h, 1+h, 2, \frac{1}{2} - \frac{1}{2\sqrt{1-4Q}}\right) \\ & \left. - 8Q(h-2) {}_2F_1\left(3-h, 1+h, 2, \frac{1}{2} - \frac{1}{2\sqrt{1-4Q}}\right) \right). \end{aligned} \tag{C.5}$$

An important point to note that this Weyl tensor square induced one point function differs from the one point function enabled by the GB coupling given in (3.19), by the polynomial factors in front of the hypergeometric functions which are not so crucial in the large  $h$  behaviour of the one point function as the more dominant contributions come from the exponential growth of the hypergeometric functions at large  $h$ .

Thus, the one point function undergoes the exact similar treatment of taking the large  $h$  limit as was illustrated in section 3 to land up into the form,

$$\langle O \rangle \sim \exp \left[ m \left( -\frac{R}{d} \log \left[ \frac{4}{\sqrt{1-4Q}} \right] + \frac{R}{d} \operatorname{arcsech}(\sqrt{1-4Q}) - i\pi \frac{R}{d} \right) \right]. \tag{C.6}$$

So, we observe that the thermal one point function due to both the Weyl tensor squared and GB coupling behaves identically at large  $h$ .

**Open Access.** This article is distributed under the terms of the Creative Commons Attribution License ([CC-BY 4.0](https://creativecommons.org/licenses/by/4.0/)), which permits any use, distribution and reproduction in any medium, provided the original author(s) and source are credited. SCOAP<sup>3</sup> supports the goals of the International Year of Basic Sciences for Sustainable Development.

## References

- [1] J.M. Maldacena, *The Large N limit of superconformal field theories and supergravity*, *Adv. Theor. Math. Phys.* **2** (1998) 231 [[hep-th/9711200](https://arxiv.org/abs/hep-th/9711200)] [[INSPIRE](https://inspirehep.net/literature/475880)].

- [2] L. Fidkowski, V. Hubeny, M. Kleban and S. Shenker, *The Black hole singularity in AdS/CFT*, *JHEP* **02** (2004) 014 [[hep-th/0306170](#)] [[INSPIRE](#)].
- [3] M. Grinberg and J. Maldacena, *Proper time to the black hole singularity from thermal one-point functions*, *JHEP* **03** (2021) 131 [[arXiv:2011.01004](#)] [[INSPIRE](#)].
- [4] D. Rodriguez-Gomez and J.G. Russo, *Correlation functions in finite temperature CFT and black hole singularities*, *JHEP* **06** (2021) 048 [[arXiv:2102.11891](#)] [[INSPIRE](#)].
- [5] B. McInnes, *The special role of toroidal black holes in holography*, *Nucl. Phys. B* **989** (2023) 116126 [[arXiv:2206.00198](#)] [[INSPIRE](#)].
- [6] G. Georgiou and D. Zoakos, *Holographic correlation functions at finite density and/or finite temperature*, *JHEP* **11** (2022) 087 [[arXiv:2209.14661](#)] [[INSPIRE](#)].
- [7] D. Berenstein and R. Mancilla, *Aspects of thermal one-point functions and response functions in AdS Black holes*, [arXiv:2211.05144](#) [[INSPIRE](#)].
- [8] J.R. David, S. Jain and S. Thakur, *Shear sum rules at finite chemical potential*, *JHEP* **03** (2012) 074 [[arXiv:1109.4072](#)] [[INSPIRE](#)].
- [9] J.R. David and S. Thakur, *Sum rules and three point functions*, *JHEP* **11** (2012) 038 [[arXiv:1207.3912](#)] [[INSPIRE](#)].
- [10] R.C. Myers, T. Sierens and W. Witczak-Krempa, *A Holographic Model for Quantum Critical Responses*, *JHEP* **05** (2016) 073 [[arXiv:1602.05599](#)] [*Addendum ibid.* **09** (2016) 066] [[INSPIRE](#)].
- [11] R. Emparan and C.P. Herzog, *Large D limit of Einstein's equations*, *Rev. Mod. Phys.* **92** (2020) 045005 [[arXiv:2003.11394](#)] [[INSPIRE](#)].
- [12] D. Giataganas, N. Pappas and N. Toumbas, *Holographic observables at large d*, *Phys. Rev. D* **105** (2022) 026016 [[arXiv:2110.14606](#)] [[INSPIRE](#)].
- [13] P. Kraus and A. Maloney, *A cardy formula for three-point coefficients or how the black hole got its spots*, *JHEP* **05** (2017) 160 [[arXiv:1608.03284](#)] [[INSPIRE](#)].
- [14] E. Witten, *Anti-de Sitter space and holography*, *Adv. Theor. Math. Phys.* **2** (1998) 253 [[hep-th/9802150](#)] [[INSPIRE](#)].
- [15] A. Sen, *Entropy function for heterotic black holes*, *JHEP* **03** (2006) 008 [[hep-th/0508042](#)] [[INSPIRE](#)].
- [16] T. Banks, M.R. Douglas, G.T. Horowitz and E.J. Martinec, *AdS dynamics from conformal field theory*, [hep-th/9808016](#) [[INSPIRE](#)].
- [17] H. Erbin, *Scalar propagators on adS space*, [https://www.lpthe.jussieu.fr/~erbin/files/ads\\_propagators.pdf](https://www.lpthe.jussieu.fr/~erbin/files/ads_propagators.pdf).
- [18] A. Chamblin, R. Emparan, C.V. Johnson and R.C. Myers, *Charged AdS black holes and catastrophic holography*, *Phys. Rev. D* **60** (1999) 064018 [[hep-th/9902170](#)] [[INSPIRE](#)].
- [19] I.S. Gradshteyn and I.M. Ryzhik, *Table of integrals, series, and products*, seventh edition, translated from Russian, translation edited and with a preface by A. Jeffrey and D. Zwillinger, Elsevier (2007).
- [20] G.N. Watson, *Asymptotic expansion of hypergeometric functions*, *Trans. Cambridge Philos. Soc.* **22** (1918) 277.

- [21] R. Emparan, *AdS membranes wrapped on surfaces of arbitrary genus*, *Phys. Lett. B* **432** (1998) 74 [[hep-th/9804031](#)] [[INSPIRE](#)].
- [22] D. Birmingham, *Topological black holes in Anti-de Sitter space*, *Class. Quant. Grav.* **16** (1999) 1197 [[hep-th/9808032](#)] [[INSPIRE](#)].
- [23] R. Emparan, *AdS/CFT duals of topological black holes and the entropy of zero energy states*, *JHEP* **06** (1999) 036 [[hep-th/9906040](#)] [[INSPIRE](#)].
- [24] H. Casini, M. Huerta and R.C. Myers, *Towards a derivation of holographic entanglement entropy*, *JHEP* **05** (2011) 036 [[arXiv:1102.0440](#)] [[INSPIRE](#)].
- [25] R. Camporesi and A. Higuchi, *Spectral functions and zeta functions in hyperbolic spaces*, *J. Math. Phys.* **35** (1994) 4217 [[INSPIRE](#)].
- [26] M. Banados, M. Henneaux, C. Teitelboim and J. Zanelli, *Geometry of the (2 + 1) black hole*, *Phys. Rev. D* **48** (1993) 1506 [[gr-qc/9302012](#)] [*Erratum ibid.* **88** (2013) 069902] [[INSPIRE](#)].
- [27] E. D'Hoker, D.Z. Freedman and L. Rastelli, *AdS/CFT four point functions: How to succeed at  $z$  integrals without really trying*, *Nucl. Phys. B* **562** (1999) 395 [[hep-th/9905049](#)] [[INSPIRE](#)].
- [28] J.M. Maldacena and A. Strominger, *AdS<sub>3</sub> black holes and a stringy exclusion principle*, *JHEP* **12** (1998) 005 [[hep-th/9804085](#)] [[INSPIRE](#)].
- [29] A. Belin, C.A. Keller and I.G. Zadeh, *Genus two partition functions and Rényi entropies of large  $c$  conformal field theories*, *J. Phys. A* **50** (2017) 435401 [[arXiv:1704.08250](#)] [[INSPIRE](#)].
- [30] L. Iliesiu, M. Kologlu, R. Mahajan, E. Perlmutter and D. Simmons-Duffin, *The Conformal Bootstrap at Finite Temperature*, *JHEP* **10** (2018) 070 [[arXiv:1802.10266](#)] [[INSPIRE](#)].
- [31] M. Dodelson, A. Grassi, C. Iossa, D. Panea Lichtig and A. Zhiboedov, *Holographic thermal correlators from supersymmetric instantons*, [arXiv:2206.07720](#) [[INSPIRE](#)].
- [32] A. Bhatta and T. Mandal, *Exact thermal correlators of holographic CFTs*, *JHEP* **02** (2023) 222 [[arXiv:2211.02449](#)] [[INSPIRE](#)].